Distinct regulation of dopamine D2S and D2L autoreceptor signaling by calcium

Stephanie C. Gantz[1], Brooks G. Robinson[1], David C. Buck[2], James R. Bunzow[1], Rachael L. Neve[3], John T. Williams[1], and Kim A. Neve[2]

[1]Vollum Institute
Oregon Health & Science University
Portland, OR 97239

[2]Research Service, VA Portland Health Care System
and
Department of Behavioral Neuroscience
Oregon Health & Science University
Portland, OR, 97239

[3]Department of Brain and Cognitive Sciences
MIT
Cambridge, MA, 02139

Corresponding author:
Kim A. Neve
Research Service, VA Portland Health Care System
R&D-30
Portland, OR, 97239
503-721-7911
nevek@ohsu.edu

The authors declare no financial competing interests.

Abstract

D2 autoreceptors regulate dopamine release throughout the brain. Two isoforms of the D2 receptor, D2S and D2L, are expressed in midbrain dopamine neurons. Differential roles of these isoforms as autoreceptors are poorly understood. By virally expressing the isoforms in dopamine neurons of D2 receptor knockout mice, this study assessed the calcium-dependence and drug-induced plasticity of D2S and D2L receptor-dependent GIRK currents. The results reveal that D2S, but not D2L receptors, exhibited calcium-dependent desensitization similar to that exhibited by endogenous autoreceptors. Two pathways of calcium signaling that regulated D2 autoreceptor-dependent GIRK signaling were identified, which distinctly affected desensitization and the magnitude of D2S and D2L receptor-dependent GIRK currents. Previous *in vivo* cocaine exposure removed calcium-dependent D2 autoreceptor desensitization in wild type, but not D2S-only mice. Thus, expression of D2S as the exclusive autoreceptor was insufficient for cocaine-induced plasticity, implying a functional role for the co-expression of D2S and D2L autoreceptors.

Introduction

Central dopamine transmission coordinates reinforcement learning, including recognition of reward-predictive stimuli and initiation of goal-directed movements. Natural rewards, reward-predictive cues, and drugs of abuse elicit a rapid increase in dopamine release from dopamine axon terminals and somatodendritic sites within the ventral midbrain. Dopamine release is negatively regulated by the activation of dopamine D2 autoreceptors on somatodendritic and axon terminals (reviewed in Ford, 2014). Loss of D2 autoreceptor-mediated inhibition results in elevated extracellular dopamine and is associated with perseverative drug-seeking, enhanced motivation for food, and novelty-induced hyperactivity (Anzalone et al., 2012; Bello et al., 2011; Holroyd et al., 2015; Marinelli and White, 2000; Marinelli et al., 2003). Chronic D2 autoreceptor activation impairs the formation of dopamine- and glutamate-releasing axon terminals (Fasano et al., 2010). Thus, D2 autoreceptors regulate structural and functional plasticity of dopamine neurons and are essential in limiting impulsivity and reward-seeking behaviors.

A prominent feature of somatodendritic D2 autoreceptors is their activation of G protein-coupled inwardly rectifying potassium (GIRK) channels, resulting in inhibition of action potential firing and subsequent dopamine release. During prolonged activation, desensitization of D2 autoreceptors reduces the D2 autoreceptor-dependent GIRK current. A component of desensitization is dependent on intracellular calcium (Beckstead and Williams, 2007). Single or repeated exposure to drugs of abuse modifies D2 autoreceptor function (Gantz et al., 2013; Henry et al., 1989; Jones et al., 2000; Madhavan et al., 2013; Marinelli et al., 2003; Wolf et al., 1993), including a loss of the calcium-dependent component of D2 autoreceptor-GIRK desensitization (Perra et al., 2011). The mechanism(s) that underlie acute desensitization and drug-induced plasticity of D2 autoreceptor-mediated inhibition remain incompletely characterized.

There are two splice variants of the D2 receptor, which differ by a 29-amino acid insert in the third intracellular loop in D2-Long (D2L) that is absent in D2-Short (D2S). Biased expression of D2S or D2L receptors alters behavioral responses to drugs of abuse (Bulwa et al., 2011; Smith et al., 2002) and has been associated with drug addiction in human studies (Moyer et al., 2011; Sasabe et al., 2007). Functionally distinct roles for D2S and D2L receptors have been proposed based on characterization of mice lacking D2L (Usiello et al., 2000; Wang et al., 2000) or D2S (Radl et al., 2013). Behavioral and biochemical studies have designated D2L as the postsynaptic receptor expressed on non-dopaminergic medium spiny neurons in the basal forebrain and D2S as the autoreceptor (Khan et al., 1998; Lindgren et al., 2003; Usiello et al., 2000). However, both D2S and D2L receptors are expressed in dopamine neurons and function as somatodendritic autoreceptors (Dragicevic et al., 2014; Jang et al., 2011; Jomphe et al., 2006; Khan et al., 1998; Neve et al., 2013). Biochemical studies indicate that D2S receptors internalize and desensitize more readily than D2L receptors (Ito et al., 1999; Itokawa et al., 1996; Liu et al., 1992; Morris et al., 2007; Thibault et al., 2011), but acute desensitization and drug-induced plasticity of D2S and D2L receptor-dependent GIRK currents have not been characterized. Using virus-mediated expression of the D2 receptor splice variants in D2 receptor knockout mice, this study reveals that D2S but not D2L receptor-dependent GIRK signaling exhibited calcium-dependent desensitization. Manipulations of pathways involved in D2 autoreceptor desensitization had distinct actions on D2S and D2L receptor-dependent GIRK currents. Lastly, a single *in vivo* cocaine exposure removed the calcium-dependent component of D2 autoreceptor-GIRK desensitization in wild type mice, but not D2S-only mice; thus, the expression of D2S as the exclusive autoreceptor was insufficient for drug-induced plasticity. Taken together, the results of this study imply a physiological role for the co-expression of D2S and D2L autoreceptors.

Results

Both D2S and D2L can function as autoreceptors

To examine the ability of D2S and D2L receptors to activate a GIRK conductance, single isoforms were expressed in midbrain dopamine neurons. *Drd2*$^{-/-}$ mice received bilateral injections of an adeno-associated viral (AAV) vector generating either rat D2S or D2L receptor and GFP expression, as previously described (Neve et al., 2013). Infected neurons in brain slices containing the substantia nigra *pars compacta* (SNc) were identified by GFP visualization. Whole-cell patch clamp recordings were made from SNc dopamine neurons using an internal solution containing the calcium chelator, BAPTA (10 mM), as used previously (Neve et al., 2013). Application of a saturating concentration of the D2 receptor agonist, quinpirole (30 μM), produced an outward current that was reversed by application of the D2 receptor antagonist, sulpiride (600 nM, Figure 1A-B). There was no difference in the peak amplitude of quinpirole-induced currents mediated by D2S and D2L receptors (Figure 1B). In the continued presence of agonist, D2 autoreceptors desensitize resulting in a decline in the agonist-induced outward current (Beckstead et al., 2009; Perra et al., 2011). The decline in the quinpirole-induced current mediated by D2S and D2L receptors was indistinguishable (Figure 1A, 1C).

In the SNc, dopamine release from neighboring dopamine neurons elicits D2 receptor-mediated inhibitory postsynaptic currents (IPSCs) through the activation of GIRK channels (Beckstead et al., 2004; Gantz et al., 2013). D2S and D2L receptors mediate kinetically-identical IPSCs following electrically stimulated dopamine release (Neve et al., 2013). Stimulus-independent dopamine release also occurs, resulting in spontaneous D2 receptor-mediated IPSCs (Gantz et al., 2013). In slices from mice infected with either D2S or D2L, spontaneous IPSCs were abolished by application of sulpiride (600 nM, Figure 1D-E). The durations of D2S, D2L, and wild type D2 receptor-mediated spontaneous IPSCs were identical (Figure 1F, [from Gantz et al., 2013, WT: 515±17 ms, n=76 sIPSCs]). Amplitude and frequency of spontaneous IPSCs are affected by the level of D2 receptor expression and dopamine synthesis (Gantz et al., 2013 and 2015). Since these parameters may be influenced by variegated viral infection, the amplitude and frequency of D2S- and D2L-sIPSCs were not compared. Taken together,

120 the results confirm previous work indicating that D2S and D2L can serve as autoreceptors at
121 somatodendritic dopamine synapses (Neve et al., 2013).
122
123 **Calcium entry promotes desensitization of D2 autoreceptors in wild type dopamine neurons**
124 Desensitization in the GIRK current induced by D2 receptor agonists is affected by intracellular
125 calcium buffering. Weak calcium buffering with intracellular EGTA (0.025 – 0.4 mM) results in
126 greater decline in the GIRK current induced by D2 receptor agonists, without affecting the decline in
127 the GIRK current induced by $GABA_B$ receptor agonists (Beckstead and Williams, 2007; Perra et al.,
128 2011). These results were confirmed in wild type mice using internal solutions containing either
129 EGTA (0.1 mM, EGTA internal) or BAPTA (10 mM, BAPTA internal). Application of quinpirole (10
130 μM) or the $GABA_B$ agonist, baclofen (30 μM), resulted in outward currents that declined in the
131 continued presence of agonist (Figure 2A, 2E). The peak amplitudes of the quinpirole- and baclofen-
132 induced currents were larger when using BAPTA internal than EGTA internal (Figure 2A-B, 2E-F).
133 The quinpirole-induced current desensitized more quickly with EGTA internal compared with
134 experiments using BAPTA internal (Figure 2A, 2C-D). This calcium-dependent desensitization was
135 specific to the D2 receptor since the decline in baclofen-induced current was not dependent on the
136 internal solution (Figure 2E, 2G-H). Thus, as reported previously (Beckstead and Williams, 2007;
137 Perra et al., 2011), D2 autoreceptors exhibited a calcium-dependent desensitization that resulted in a
138 larger decline in the D2 autoreceptor-dependent current when intracellular calcium was buffered with a
139 low concentration of EGTA.
140 EGTA and BAPTA have a similar affinity for calcium but differ in the kinetics of binding. This
141 property is frequently used to characterize the distance between a calcium source and a calcium sensor.
142 Buffering with EGTA allows calcium to diffuse farther (microdomain) than BAPTA, which limits
143 calcium spread (nanodomain) from a calcium source. However, the concentrations of EGTA and
144 BAPTA used in this study may also result in different levels of resting free calcium (Adler et al.,

1991). To determine whether the difference in D2 autoreceptor desensitization observed with the two internals was explained by resting free calcium concentration, the level of free calcium in the BAPTA internal was increased to 300 nM by addition of $CaCl_2$ (7.37 mM) (BAPTA+Ca^{2+}, see Materials and Methods). The peak amplitude and the decline in the quinpirole-induced current recorded with BAPTA+Ca^{2+} internal were not different from measurements recorded with BAPTA alone (Figure 3A-B). Interestingly, BAPTA+Ca^{2+} internal decreased the peak amplitude of the baclofen-induced current significantly relative to the amplitude recorded with BAPTA internal (Figure 3C), and was not different from the current measured with EGTA internal (Figure 3C). The decline in the baclofen-induced current was unaffected by BAPTA+Ca^{2+} (Figure 3D).

To verify that the resting free calcium was increased using BAPTA+Ca^{2+} internal, the positive modulator of the small conductance calcium-activated potassium channel (SK), NS309 (10 μM) was applied. Although NS309 did not produce a current using either BAPTA or EGTA internals, it caused an outward current with BAPTA+Ca^{2+} internal (Figure 3-figure supplement 1A-B). The NS309-induced current was reversed by the SK channel blocker apamin (200 nM). Thus, the BAPTA+Ca^{2+} internal increased resting free calcium.

Taken together, the results indicate that the resting free calcium had differential actions on D2 and $GABA_B$ receptor-dependent GIRK currents. The magnitude of the $GABA_B$ receptor-dependent current was sensitive to resting free calcium, but the decline in current was independent of resting free calcium. The decline in D2 autoreceptor-dependent current was dominated by the spatial regulation of intracellular calcium, not resting free calcium.

Desensitization of D2S- but not D2L-GIRK currents is calcium-dependent

Recordings were made from dopamine neurons that expressed D2S or D2L receptors using an internal solution containing EGTA (0.1 mM). Application of quinpirole (30 μM) produced an outward current that declined and was reversed by sulpiride (600 nM). In D2S neurons, the decline using EGTA

internal was faster than the decline using BAPTA internal (Figure 4A, 4D, Figure 4 - figure supplement 1A). In contrast, in D2L neurons, the decline with EGTA and BAPTA internal was not different (Figure 4A, 4D, Figure 4 - figure supplement 1B). The insensitivity of the decline in D2L neurons to calcium buffering resulted in significantly more desensitization of D2S than D2L with EGTA internal (Figure 4B). The peak amplitude of the quinpirole-induced currents in D2S and D2L neurons was not different (Figure 4C), indicating the difference between D2S and D2L is unlikely to be due to differences in the level of expression of D2 receptors. Application of the $GABA_B$ agonist, baclofen (30 μM), produced an outward current that was reversed by the $GABA_B$ antagonist, CGP-55845 (200 nM). The peak amplitude of the baclofen-induced current was not different among D2S (EGTA: 259±28 pA; BAPTA: 531±94 pA), D2L (EGTA: 277±29 pA; BAPTA: 520±43 pA), D2-KO (AAV-GFP-only, EGTA: 279±54 pA; BAPTA: 664±80 pA), and wild type dopamine neurons ($p>0.05$). There was also no change in the decline in the baclofen-induced current in D2S- or D2L-expressing neurons (Figure 4E).

To minimize potential confounds of ectopic D2 receptor expression in non-dopamine neurons in the midbrain, the calcium-sensitivity of D2S receptor-GIRK desensitization was validated using a transgenic D2-Short mouse line, generated by a cross between TH-hD2S (Gantz et al., 2013) and D2 receptor knockout mice. In this line, the expression of Flag-tagged human D2S receptors depends on the tyrosine hydroxylase promoter (Figure 4 - figure supplement 2). In slices from these mice, quinpirole (10 μM) produced larger outward currents using BAPTA internal compared to EGTA internal (Figure 4F). The currents were significantly larger than those recorded in wild type dopamine neurons (Figure 2B, 4F), indicating overexpression of D2 receptors. Despite the overexpression, the magnitude of the decline in the quinpirole-induced current was similar to wild type (Figure 2C-D, 4H). Also consistent with wild type, the decline in the quinpirole-induced current using EGTA internal was significantly faster than the decline using BAPTA internal (Figure 4G-H). Taken together, these results indicate that D2S but not D2L receptor-GIRK signaling exhibited calcium-dependent desensitization.

Calcium signaling regulates D2 autoreceptor-activated GIRK conductance

Intracellular calcium stores

Endoplasmic calcium stores contribute to calcium-dependent desensitization of D2 autoreceptor-GIRK signaling (Perra et al., 2011). Cyclopiazonic acid (CPA) disrupts the sarco/endoplasmic reticulum calcium-ATPase leading to rapid depletion of intracellular calcium stores (Ford et al., 2010). Brain slices were exposed to CPA (10 μM) >20 min prior to making recordings. As shown previously in wild type dopamine neurons, CPA reduced the decline in the quinpirole-induced current using EGTA internal and had no effect when using BAPTA internal (Figure 5A). CPA did not change the decline in the baclofen-induced current recorded with either internal (Figure 5B). In D2S neurons, CPA also reduced the decline in the quinpirole-induced current, but the decline in the quinpirole-induced current in D2L neurons was not changed (Figure 5C). These results indicate that calcium release from intracellular stores contributed to D2S but not D2L receptor-GIRK desensitization.

In wild type neurons with EGTA internal, CPA had no significant effect on the magnitude of the maximal current produced by bath application of quinpirole (control: 172±19 pA, n=15; CPA: 194±22 pA, n=13, p=0.46, unpaired t test). In a previous study, sub-saturating D2 receptor-dependent currents repeatedly produced by pressure ejection of dopamine are augmented by bath application of CPA for 10-20 min (Perra et al., 2011). Therefore, the effect of CPA was examined on submaximal dopamine currents produced by iontophoretic application of dopamine once every 50 s (I-DA). In wild type neurons using an EGTA internal, CPA (10 μM) significantly augmented I-DA (Figure 5D). While CPA rapidly depletes intracellular calcium stores, the CPA-induced augmentation of I-DA did not plateau until >15 min (Figure 5-figure supplement 1). CPA also significantly augmented I-DA in D2S and D2L neurons (Figure 5E and Figure 5 – figure supplement 1). However, the magnitude of the increase was significantly greater for D2L receptor-dependent currents than D2S (Figure 5E). Thus,

depletion of calcium from intracellular stores differentially increased D2S and D2L receptor-dependent GIRK signaling.

L-type calcium channels

In SNc dopamine neurons, calcium entry via somatodendritic low-voltage-activated L-type calcium channels occurs during tonic 'pacemaker' action potential firing, creating oscillations of elevated cytosolic calcium in the somatodendritic compartment (Chan et al., 2007; Hage and Khaliq, 2015; Puopolo et al., 2007). L-type calcium channels may be involved in D2 autoreceptor desensitization, (Dragicevic et al., 2014; Goldberg et al., 2005; Guzman et al., 2010), but no studies have directly measured D2 autoreceptor-dependent GIRK signaling. To determine if L-type calcium channels regulate D2 autoreceptor-dependent GIRK signaling, brain slices were exposed to the L-type calcium channel blocker, isradipine (300 nM), >20 min prior to making recordings. In wild type dopamine neurons, isradipine did not significantly change the decline in the quinpirole-induced current using either EGTA or BAPTA internal (Figure 6A). Isradipine also had no effect on the decline in baclofen-induced current (Figure 6B). However, isradipine reduced the decline in the quinpirole-induced current in D2S neurons, without affecting the decline in D2L neurons (Figure 6C). Taken together, the results suggest that calcium influx via L-type calcium channels was not involved in desensitization of D2 autoreceptor-dependent GIRK currents in wild type dopamine neurons, but promoted desensitization of D2S receptors.

In wild type neurons with EGTA internal, isradipine had no significant effect on the magnitude of the maximal current produced by bath application of quinpirole (control: 172±19 pA, n=15; israd: 178±28 pA, n=11, p=0.86, unpaired t test). Therefore, the effect of isradipine on I-DA was examined. In wild type dopamine neurons using an EGTA internal, isradipine (300 nM) significantly augmented I-DA (Figure 6D) after >10 min (Figure 6-figure supplement 1). In D2S and D2L neurons, I-DA was also augmented by isradipine (Figure 6E and Figure 6-figure supplement 1). As was found with CPA,

244 the magnitude of the increase was greater for D2L receptor-dependent currents than D2S (Figure 6E).
245 Thus, inhibition of calcium entry via L-type calcium channels differentially increased D2S and D2L
246 receptor-dependent GIRK signaling.
247
248 **A single *in vivo* cocaine exposure decreases calcium-dependent D2 autoreceptor desensitization**
249 Drugs of abuse change the D2 autoreceptor activation of GIRK conductance (Arora et al., 2011;
250 Beckstead and Williams, 2007; Dragicevic et al., 2014; Gantz et al., 2013; Sharpe et al., 2014). One of
251 these changes is a loss of the calcium-dependent component of D2 autoreceptor desensitization after
252 repeated ethanol exposure (Perra et al., 2011). Wild type mice were given a single injection of cocaine
253 (20 mg/kg, i.p.) or an equal volume of saline, and brain slices were made 24 h later. With EGTA
254 internal, the quinpirole-induced current declined significantly less in slices from cocaine-treated mice
255 compared to control mice (saline-treated and naïve, Figure 7A). In fact, the decline was no longer
256 statistically different from that found with BAPTA internal (Figure 7A). There was no difference in the
257 decline in the quinpirole-induced current in slices taken from control or cocaine-treated mice with
258 BAPTA internal (Figure 7A). There was no change in the decline in the baclofen-induced current,
259 using either internal (Figure 7F). Thus, in wild type mice, a single *in vivo* cocaine exposure resulted in
260 the loss of calcium-dependent D2 autoreceptor desensitization without affecting $GABA_B$ receptor
261 desensitization.
262 A loss of calcium-dependent D2 autoreceptor desensitization after cocaine exposure in wild
263 type neurons could be due to a change in calcium signaling or a functional increase in the contribution
264 of D2L receptors. To test whether D2L receptors are involved, *Drd2*$^{-/-}$ mice that had received
265 midbrain injections of AAV-D2S or AAV-D2L were given a single injection of cocaine (20 mg/kg,
266 i.p.) and brain slices were made 24 h later. In D2L neurons, cocaine exposure did not alter the decline
267 in quinpirole-induced current (Figure 7B). Likewise, cocaine exposure did not alter the calcium-
268 dependent decline in the quinpirole-induced current in D2S neurons. Similar to naïve AAV-D2S mice,

the decline of the quinpirole-induced current was greater using EGTA internal than with BAPTA internal (Figure 7C). Thus, unlike what was found in slices from wild type mice, cocaine exposure did not reduce the calcium-dependent decline in the quinpirole-induced current. This result was not dependent on overexpression as it was also observed in D2S neurons in which quinpirole produced outward currents of similar magnitude to wild type neurons (data not shown). This result was also recapitulated in the transgenic D2-Short mice (Figure 7D), where expression of D2S receptors in the midbrain is restricted to dopamine neurons. Since wild type, but not D2S-only dopamine neurons exhibited a reduction in calcium-dependent desensitization after cocaine exposure, these results suggest that constitutive or viral-mediated expression of D2S as the exclusive autoreceptor was insufficient for cocaine-induced plasticity.

To determine if the expression of D2L was sufficient to enable loss of calcium-dependent D2 receptor desensitization of D2S, *Drd2*$^{-/-}$ mice received bilateral injections of a 1:1 mixture of AAV-D2S and AAV-D2L. In dopamine neurons from mice infected with both splice variants, the amplitude of the quinpirole-induced currents was similar to those measured in neurons expressing D2S- or D2L-only (EGTA: 333±48 pA, n=9; BAPTA: 442±86 pA, n=6, see Figures 1B and 4C for comparison). This suggests a similar level of D2 receptor overexpression as in neurons that express single variants. Surprisingly, the decline in the quinpirole-induced current was similar between EGTA and BAPTA internals (Figure 7E). Therefore, the viral expression of both D2S and D2L receptors did not mimic D2 receptor-dependent GIRK signaling in naïve wild type mice. Moreover, the decline in the quinpirole-induced current did not change after *in vivo* cocaine exposure (Figure 7E), suggesting that the viral expression of both D2S and D2L receptors precluded cocaine-induced plasticity in D2 receptor-dependent GIRK signaling. To ensure that this result was not due to preferential expression of D2L receptors following injection of the D2S/D2L virus mixture, dopamine neurons in transgenic D2-Short mice were infected with AAV-D2L. The expression of D2S was confirmed by labeling dopamine neurons with an Alexa Fluor 594-conjugated M1 antibody and imaging on a two-photon microscope

(e.g. Figure 4 - figure supplement 2B). Recordings were made from neurons with Flag-D2S staining that were also GFP^+ (AAV-D2L). With EGTA internal, the decline in the quinpirole-induced current in transgenic D2-Short neurons also expressing D2L was equivalent to the decline measured in neurons receiving the D2S/D2L virus mixture, and significantly less than the decline in the quinpirole-induced current in transgenic D2-Short-only neurons (Figure 7D). As observed in wild type, there was no change in the decline in the baclofen-induced current after cocaine exposure in any of the groups ($p>0.05$ for all comparisons, data not shown). Taken together, the results indicate that regardless of the presence of D2S, the viral expression of D2L eliminated calcium-dependent D2 receptor desensitization and precluded cocaine-induced plasticity.

Discussion

Alternative splicing generates two isoforms of the dopamine D2 receptor, D2S and D2L. D2S has been considered the autoreceptor, but both are expressed and functional in midbrain dopamine neurons. Evidence of distinct functional roles for the splice variants as autoreceptors has not been described. This study assessed the calcium-dependence and drug-induced plasticity of the desensitization of GIRK currents mediated by D2S and D2L receptors expressed in SNc dopamine neurons. The results reveal that the D2S receptor, but not the D2L receptor, exhibited calcium-dependent desensitization. Manipulating pathways for calcium signaling removed the calcium-dependent component of D2S receptor desensitization, demonstrating these receptors were amenable to plasticity. Cocaine exposure eliminated calcium-dependent D2 autoreceptor desensitization in dopamine neurons from wild type mice without altering desensitization of neurons expressing only D2S or D2L. Furthermore, viral expression of D2L eliminated calcium-dependent desensitization, resembling the D2 autoreceptor desensitization observed in dopamine neurons from wild type mice after *in vivo* cocaine exposure.

Calcium-dependent regulation of D2 autoreceptor-dependent GIRK conductance

Calcium entry promotes desensitization of D2 autoreceptors in wild type dopamine neurons. Buffering intracellular calcium with BAPTA reduces the decline in D2 autoreceptor-, but not $GABA_B$ receptor-mediated GIRK currents (Beckstead and Williams, 2007; Perra et al., 2011). In this study, the calcium-dependent component of D2 autoreceptor desensitization was observed in wild type and D2S-only expressing dopamine neurons. However, in neurons where D2L receptors were virally expressed, there was no calcium-dependent desensitization. This was observed whether D2L receptors were expressed alone, or in conjunction with transgenic or virally expressed D2S receptors.

This study describes two calcium sources that regulate D2 autoreceptor-dependent GIRK currents: intracellular calcium stores and L-type calcium channels. These intracellular pathways did not regulate desensitization of $GABA_B$ receptor-dependent GIRK currents. Consistent with a previous report (Perra et al., 2011), depleting intracellular calcium stores removed calcium-dependent D2 autoreceptor desensitization in wild type neurons. Depleting intracellular calcium stores also reduced the magnitude of D2S receptor desensitization to a saturating concentration of agonist, without affecting D2L receptor desensitization. Preventing calcium entry from L-type calcium channels also reduced D2S receptor desensitization, without affecting wild type or D2L receptor desensitization. The results demonstrate that the calcium-dependent component of D2S receptor desensitization was readily modifiable.

Desensitization of D2 autoreceptors in wild type dopamine neurons was controlled by elevated concentrations of calcium in intracellular microdomains and could not be enhanced by raising the resting free calcium concentration. The lack of a calcium-dependent component in D2L receptor desensitization could be due to localization outside of the calcium microdomains, despite showing similar distribution in the somatodendritic compartment as D2S receptors (Jomphe et al., 2006), or to another property of this isoform. Depleting intracellular calcium stores or blocking L-type calcium channels produced robust augmentation in D2L receptor-dependent GIRK currents produced by

iontophoretically applied dopamine that was greater than the augmentation of D2S receptor-dependent GIRK currents. The lack of effect of manipulating calcium signaling on D2L receptor desensitization in the presence of a saturating concentration of quinpirole suggests that the enhanced response of D2L to iontophoretically applied dopamine does not reflect removal of tonic desensitization. Nonetheless, the same intracellular pathways interacting with D2S receptors also modified D2L receptor-dependent GIRK currents. It is therefore likely that D2S and D2L receptors are in similar calcium microdomains and the lack of apparent calcium-dependent desensitization upon saturating agonist exposure is a property specific to the D2L isoform.

Plasticity of the calcium-dependent D2 autoreceptor desensitization

Drugs of abuse cause functional changes to dopamine neuron physiology, including regulation of D2 and $GABA_B$ receptor activation of GIRK conductance (Arora et al., 2011; Beckstead et al., 2009; Dragicevic et al., 2014; Padgett et al., 2012; Perra et al., 2011; Sharpe et al., 2014). Several recent studies reported drug-induced changes in D2 autoreceptor mediated-GIRK signaling that are contingent on the method of recording (whole-cell versus perforated-patch, Dragicevic et al., 2014) or the calcium buffering capabilities of the whole-cell internal solution (Perra et al., 2011; Sharpe et al., 2014) implicating dependence on intracellular calcium. In this study, 24 h after a single *in vivo* cocaine exposure, the calcium-dependent component of D2 autoreceptor desensitization was eliminated, similar to the change observed after repeated ethanol exposure (Perra et al., 2011). Thus, this study confirms the Perra et al. (2011) finding and further demonstrates that the plasticity in D2 autoreceptor function did not require repeated drug exposure. Whether this plasticity was due to a change in calcium-dependent pathways or the D2 autoreceptors themselves was previously unresolved. The findings of this study support the latter.

Cocaine exposure may change the calcium-dependent pathways examined in this study. Twenty-four h after a single cocaine exposure, metabotropic glutamate receptor 1 signaling is

368 attenuated (Kramer and Williams, 2015). The activation of metabotropic glutamate receptors decreases
369 D2 autoreceptor-dependent GIRK currents (Perra et al., 2011) and may desensitize D2 autoreceptors
370 through calcium release from intracellular stores. A change in the contribution of calcium influx via L-
371 type calcium channels to D2 autoreceptor desensitization may also result from cocaine exposure
372 (Dragicevic et al., 2014). In this study, depleting intracellular calcium stores or blocking L-type
373 calcium channels readily removed calcium-dependent D2S receptor desensitization. Given these
374 results, it was surprising that cocaine exposure did not alter calcium-dependent D2S receptor
375 desensitization. This result was recapitulated in dopamine neurons from transgenic D2-Short mice
376 indicating it was not an artifact of virus-mediated expression. Thus, these results suggest that the
377 expression of D2S as the exclusive autoreceptor is insufficient for cocaine-induced plasticity observed
378 in wild type dopamine neurons.

379 In wild type dopamine neurons, it may be that the expression of D2L receptors is involved in
380 cocaine-induced plasticity. Biased expression of D2S and D2L receptors has been associated with drug
381 abuse. The loss of D2L receptors and concomitant overexpression of D2S receptors in D2L-deficient
382 mice is associated with altered drug-taking (Bulwa et al., 2011) and conditioned place preference
383 (Smith et al., 2002). In addition, single nucleotide polymorphisms that result in overexpression of D2S
384 receptors are observed in humans with a history of drug abuse (Moyer et al., 2011; Sasabe et al., 2007).
385 In this study, the viral expression of D2L receptors, alone or with D2S receptors, resulted in a loss of
386 calcium-dependent D2 receptor desensitization. Moreover, it precluded any further cocaine-induced
387 reduction in calcium-dependent D2 receptor desensitization. These results suggest that the
388 overexpression of D2L receptors resembles cocaine-induced plasticity. Transient elevation in
389 extracellular dopamine up-regulates D2L mRNA (Giordano et al., 2006; Oomizu et al., 2003;
390 Wernicke et al., 2010; Zhang et al., 1994; but see Dragicevic et al., 2014; Filtz et al., 1993). In
391 addition, D2L receptors are retained in intracellular compartments more so than D2S receptors and
392 exposure to D2 agonists results in the preferential translocation of existing and nascent D2L receptors

393 to the membrane (Filtz et al., 1993; Ng et al., 1997; Starr et al., 1995; Zhang et al., 1994; Fishburn et
394 al., 1995; Prou et al., 2001). Thus, it may be that exposure to cocaine in wild type mice increases
395 functional D2L receptors, resulting in the loss of calcium-dependent D2 autoreceptor desensitization.
396 Virally expressed D2L receptors may not be subject to the same regulation as endogenously expressed
397 D2L receptors, in such a way that virus-mediated overexpression of D2L mimics and eliminates any
398 requirement for up-regulation of D2L function.
399
400 **Both D2S and D2L function as autoreceptors**
401 The D2S isoform has been thought to be the D2 autoreceptor due to preservation of autoreceptor-
402 mediated behaviors in D2L-deficient mice and more abundant D2S immunolabeling in the SNc (Khan
403 et al., 1998; Usiello et al., 2000). However, immunolabeled D2L receptors are found in SNc dopamine
404 neurons (Khan et al., 1998) and rodent studies describe dopamine neurons expressing both D2S and
405 D2L mRNA, D2L-only, or D2S-only (Dragicevic et al., 2014; Jang et al., 2011). Both variants are
406 capable of inhibiting action potential firing (Dragicevic et al., 2014; Jang et al., 2011; Jomphe et al.,
407 2006). In this study, D2S and D2L receptors, when expressed in dopamine neurons, activated a GIRK
408 conductance and were capable of producing IPSCs occurring from spontaneous fusion of dopamine-
409 filled vesicles. Thus, D2S and D2L can serve as autoreceptors at somatodendritic dopamine synapses,
410 as previously demonstrated (Neve et al., 2013).
411 Although many of the basic properties of D2S and D2L receptor-dependent currents were
412 similar, there were some differences that suggest both D2S and D2L are autoreceptors in wild type
413 dopamine neurons. The calcium-dependent component of D2 autoreceptor desensitization in wild type
414 neurons was similar to D2S-only neurons. However, results from manipulating calcium signaling in
415 wild type neurons were more consistent with a mix of D2S and D2L receptor expression. Intracellular
416 pathways for calcium signaling that regulated D2S receptor-GIRK desensitization modified the
417 magnitude of D2L receptor-dependent GIRK currents. In wild type dopamine neurons, manipulating

these pathways resulted in a decrease in acute desensitization and larger GIRK currents, suggesting that D2S and D2L receptor regulation may operate in parallel in wild type neurons. In addition, cocaine-induced plasticity occurred in wild type, but not D2S-only neurons, indicating a loss of some process in neurons which express D2S as the exclusive autoreceptor that is not permissive to cocaine-induced plasticity. However, the viral-mediated co-expression of D2S with D2L receptors also did not resemble wild type, and instead was similar to D2L-only. Although it is not known to what extent developmental compensation, virus-mediated expression, and variegated D2 receptor expression in *Drd2*$^{-/-}$ mice affected D2 receptor translation or trafficking (i.e. affecting the ratio of functional D2S and D2L receptors), or other regulatory elements of D2 receptor signaling, this result suggests that in wild type dopamine neurons, the functional expression of D2L may be limited. Changes in calcium signaling or exposure to cocaine may bring about an increased contribution of D2L, although this has yet to be directly demonstrated. Taken together, this study suggests that D2S may serve as the predominant autoreceptor under basal conditions, but the functional contribution of D2L autoreceptors may be revealed after drug exposure.

Concluding remarks

This study advances the understanding of D2 autoreceptor regulation. Two pathways for calcium signaling that regulated D2 autoreceptor-dependent GIRK signaling were identified, which distinctly affected D2S and D2L receptors. In addition, distinct action of *in vivo* cocaine exposure in wild type, D2S, and D2L receptor-GIRK signaling was demonstrated. Since not all dopamine neurons express both D2S and D2L receptors, this study suggests that D2 autoreceptors in a subset of dopamine neurons are regulated differently by calcium and resistant to cocaine-induced plasticity. Given the heterogeneity of dopamine neurons and their projections (reviewed in Roeper, 2013), a greater understanding of this subset may reveal insights into plasticity in their projection areas.

Materials and Methods

Animals

All studies were conducted in accordance with the Institutional Animal Care and Use Committees at the VA Portland Health Care System (VAPORHCS) and Oregon Health & Science University (OHSU). Mice of both sexes were used in this study (65-120 days old). Wild type (C57BL/6) mice, obtained from The Jackson laboratory, and TH-hD2S mice were bred at OHSU. *Drd2*$^{-/-}$ mice were bred at the VAPORHCS Veterinary Medical Unit and were maintained on a C57BL/6 background. Mice were housed in standard plastic containers on a 12-hour light/dark cycle. Food and water were available *ad libitum*, and after stereotaxic injections, diet was supplemented with Diet Gel RE placed on the floor of the cage. "Transgenic D2-Short" mice were produced by crossing *Drd2*$^{-/-}$ mice with transgenic TH-hD2S mice which express Flag-tagged human D2S receptors, under the tyrosine hydroxylase promoter (Gantz et al., 2013), as shown by immunostaining for the Flag epitope with an Alexa Fluor 594-conjugated M1 antibody and confocal or two-photon microscopy (Figure 4 – supplement 2). Treated animals received one injection of cocaine (20 mg/kg, intraperitoneally) dissolved in saline, or an equal volume of saline, 22-24 h prior to use. There were no differences found between saline-treated and naïve mice, so data were combined.

Stereotaxic Injections and Viruses

D2 receptors were ubiquitously expressed in the midbrain using an adeno-associated viral (AAV) vector (AAV9 D2-IRES-GFP; Virovek, Inc.) encoding rat D2S or D2L receptors (Neve et al., 2013), or a 1:1 mixture of AAV-D2S and AAV-D2L. Mice were injected when 65-90 days old. Mice were immobilized in a stereotaxic alignment system under an anesthesia cocktail consisting of 7.1 mg/kg xylazine, 71.4 mg/kg ketamine, and 1.4 mg/kg acepromazine (10 ml/kg). Mice received bilateral injections, each 500 nl volume at a rate of 200 nl/min, with the injection needle left in place for an

467 additional 5 min before it was slowly withdrawn. The coordinates for injections were (with respect to
468 bregma) AP -3.26 mm, ML ±1.2 mm, DV -4.0 mm. After injections, mice recovered in individual or
469 group housing for 3-4 weeks to allow for expression. Infected neurons were identified in the slice by
470 visualization of eGFP.
471
472 **Slice Preparation and Electrophysiology**
473 Whole-cell voltage clamp recordings (holding potential -60 mV) were made as previously described
474 (Gantz et al., 2013). Whenever possible, experiments were conducted blinded to treatment or splice
475 variant expression. Mice were deeply anesthetized with isoflurane and killed by decapitation. Brains
476 were removed quickly and placed in ice-cold physiologically equivalent saline solution (modified
477 Krebs buffer) containing (in mM) 126 NaCl, 2.5 KCl, 1.2 $MgCl_2$, 2.4 $CaCl_2$, 1.4 NaH_2PO_4, 25
478 $NaHCO_3$, and 11 D-glucose with MK-801 (10 μM), and cut horizontally (220 μm) using a vibrating
479 microtome (Leica). Slices recovered at 30 ºC in vials with 95/5% O_2/CO_2 saline with MK-801 (10 μM)
480 for at least 30 min prior to recording. Slices were then mounted in a recording chamber and perfused at
481 a rate of ~3.0 ml/min with 33-35.5 ºC modified Krebs buffer. Recordings were made exclusively from
482 neurons in the substantia nigra *pars compacta* (SNc) identified visually by their location lateral to the
483 medial terminal nucleus of the accessory optic. The neurochemical identity of AAV-D2-infected cells
484 was not verified post-recording. Rather, dopamine neurons were identified by location and
485 electrophysiological properties, namely the presence of spontaneous pacemaker firing of broad (~2 ms)
486 action potentials at 1-5 Hz in cell-attached mode (Ford et al., 2006), characteristic passive membrane
487 properties including capacitance and resting conductance (Gantz et al., 2011), and a prominent slow
488 hyperpolarization-activated inward (I_h) current (Ford et al., 2006). These parameters readily
489 distinguished dopamine neurons from GABAergic neurons. The expression of D2 receptors was not
490 used as a physiological criterion for dopamine neuron identity. However, all dopamine neurons from

491 wild type mice identified by location and electrophysiological properties had a D2 receptor-dependent
492 outward current upon quinpirole application. Recordings were obtained with large glass electrodes
493 with a resistance of 1.3-1.9 MΩ when filled with internal solution containing either, (in mM) 115 K-
494 methanesulfonate, 20 NaCl, 1.5 $MgCl_2$, 10 HEPES (K), 2 ATP, 0.2 GTP, 10 phosphocreatine, and 10
495 BAPTA (K4) or 130 K-methanesulfonate, 20 KCl, 1 $MgCl_2$, 10 HEPES (K), 2 ATP, 0.2 GTP, 10
496 phosphocreatine, and 0.1 EGTA; pH 7.33-7.40, 275-288 mOsm. The concentration of $CaCl_2$ required
497 to increase resting free calcium in BAPTA internal was determined with use of the EGTAetc program,
498 provided by E.W. McCleskey. Within 2 min of break-in, membrane capacitance, series resistance, and
499 input resistance were measured with the application of 3 pulses (±2 mV for 50 ms) averaged before
500 computation using the Axograph (sampled at 50 kHz, filtered at 10 kHz). Series resistance was
501 monitored to ensure sufficient and stable electrical access to the inside of the cell throughout the
502 experiment (<12 MΩ). Cells were dialyzed with internal solution for >10 min prior to drug application
503 (Foehring et al., 2009). All drugs were applied through bath perfusion, except dopamine, which was
504 applied by iontophoresis. Quinpirole and baclofen were applied with >10 min between the agonist
505 applications with the application order alternated between recordings. The amplitude and the decline in
506 the currents were not affected by the order in which the drugs applied. Slices were exposed to
507 saturating concentrations of each agonist once. Recordings where the peak amplitude of the current
508 was <50 pA were excluded from decline analysis. Dopamine hydrochloride (1 M) was ejected as a
509 cation with a single pulse (2-10 ms, >20 nA) from a thin-walled iontophoretic electrode placed with 10
510 μm of the soma once every 50 s. Access resistance was assessed during these recordings with a brief
511 (200 ms) step to -70 mV once every 50 s. Data were acquired using AxoGraph software (AxographX)
512 and Chart 7 (AD Instruments) and were post-hoc filtered. The amplitude of currents induced by
513 iontophoretic application of dopamine was determined by averaging the current±20 ms from the
514 greatest upward deflection. For each cell, 6-24 consecutive currents were averaged to determine
515 'baseline' (preceding drug application) and post-drug amplitudes. sIPSCs were detected and analyzed

as previously described (Gantz et al., 2013). Briefly, single peak sIPSCs with amplitudes greater than 2.1 times the SD of baseline noise were detected using a semiautomated sliding template detection procedure with AxoGraph X. Each detected event was visually inspected and discarded if the baseline noise was greater than the sIPSC peak ±1 s from the peak. Duration of sIPSCs was determined by measuring the width at 20% of the peak.

Flag-D2S receptor immunohistochemistry and microscopy

Brain slices were prepared and allowed to recover, as described for electrophysiology. Slices were incubated in Alexa Fluor 594-conjugated M1 antibody (10 µg/ml) for 40 min at 35 ºC. Live slices were observed with a custom-built two-photon microscope using *ScanImage* Software (Pologruto et al., 2003). Expression of eGFP was visualized using a CCD camera of epi-fluorescence activation. Slices for laser-scanning confocal microscopy were washed 10 min in modified Krebs buffer before fixation in 4% paraformaldehyde (45 min at 24 ºC) in phosphate buffered saline + $CaCl_2$ (1 mM, PBS+Ca^{2+}). Slices were blocked and permeabilized in PBS+Ca^{2+} with 0.3% Triton-X and 0.5% fish skin gelatin for 80 min. Slices were incubated overnight in rabbit anti-tyrosine hydroxylase antibody (1:1000 in PBS+Ca^{2+} + 0.05% NaN_3). Washed slices were incubated in Alexa Fluor 488-conjugated goat anti-rabbit secondary antibody (1:1000 in PBS+Ca^{2+} + 0.05% NaN_3, 2 h at 24 ºC). Washed slices were mounted with Fluoromount aqueous medium with #1.5 glass coverslips. Images were collected on a Zeiss confocal LSM 780 microscope with a 40x water-emersion lens (1.2 nA). All images were processed with Fiji.

Materials

CGP-55845 was obtained from Tocris Bioscience. MK-801 and cyclopiazonic acid were obtained from Abcam. Cocaine hydrochloride was obtained from National Institute on Drug Abuse-National Institutes of Health (Bethesda, MD, USA). All other drugs were obtained from Sigma-Aldrich.

Statistical analyses

Values are given as means±SEM and unless otherwise noted n=number of cells. Data sets with $n>10$ were tested for normality with a Shapiro-Wilk test. Significant between-group differences were determined in two group comparisons by unpaired two-tailed *t* tests or Mann Whitney U tests, and in more than two groups comparisons by one- or two-way ANOVAs. ANOVAs were followed when $p<0.05$ with uncorrected Fisher's LSD or Bonferroni's multiple comparisons *post hoc* tests. Significant differences in within-group comparisons were determined by paired two-tailed *t* tests. Statistical analysis was performed using GraphPad Prism 6 (GraphPad Software, Inc.).

Acknowledgments

This work was supported by the Merit Review Award BX000810 from the US Department of Veterans Affairs, Veterans Health Administration, Office of Research and Development, Biomedical Laboratory Research and Development (K.A.N.) and by NIH P50 DA018165 (K.A.N.), F32 DA038456 (B.G.R), DA04523 (J.T.W.), and DA034388 (J.T.W.).

References

Adler, E.M., Augustine, G.J., Duffy, S.N., and Charlton, M.P. (1991). Alien intracellular calcium chelators attenuate neurotransmitter release at the squid giant synapse. J Neurosci *11*, 1496–1507.

Anzalone, A., Lizardi-Ortiz, J.E., Ramos, M., De Mei, C., Hopf, F.W., Iaccarino, C., Halbout, B., Jacobsen, J., Kinoshita, C., Welter, M., et al. (2012). Dual Control of Dopamine Synthesis and Release by Presynaptic and Postsynaptic Dopamine D2 Receptors. Journal of Neuroscience *32*, 9023–9034.

Arora, D., Hearing, M., Haluk, D.M., Mirkovic, K., Fajardo-Serrano, A., Wessendorf, M.W., Watanabe, M., Luján, R., and Wickman, K. (2011). Acute cocaine exposure weakens GABA(B) receptor-dependent G-protein-gated inwardly rectifying K+ signaling in dopamine neurons of the ventral tegmental area. Journal of Neuroscience *31*, 12251–12257.

Beckstead, M.J., and Williams, J.T. (2007). Long-Term Depression of a Dopamine IPSC. J Neurosci *27*, 2074–2080.

Beckstead, M.J., Gantz, S.C., Ford, C.P., Stenzel-Poore, M.P., Phillips, P.E., Mark, G.P., and

570 Williams, J.T. (2009). CRF enhancement of GIRK channel-mediated transmission in dopamine
571 neurons. Neuropsychopharmacology *34*, 1926–1935.

572 Beckstead, M.J., Grandy, D.K., Wickman, K., and Williams, J.T. (2004). Vesicular Dopamine Release
573 Elicits an Inhibitory Postsynaptic Current in Midbrain Dopamine Neurons. Neuron *42*, 939–946.

574 Bello, E.P., Mateo, Y., Gelman, D.M., Noaín, D., Shin, J.H., Low, M.J., Alvarez, V.A., Lovinger,
575 D.M., and Rubinstein, M. (2011). Cocaine supersensitivity and enhanced motivation for reward in
576 mice lacking dopamine D2 autoreceptors. Nature Publishing Group *14*, 1033–1038.

577 Bulwa, Z.B., Sharlin, J.A., Clark, P.J., Bhattacharya, T.K., Kilby, C.N., Wang, Y., and Rhodes, J.S.
578 (2011). Increased consumption of ethanol and sugar water in mice lacking the dopamine D2 long
579 receptor. Alcohol *45*, 631–639.

580 Chan, C.S., Guzman, J.N., Ilijic, E., Mercer, J.N., Rick, C., Tkatch, T., Meredith, G.E., and Surmeier,
581 D.J. (2007). "Rejuvenation" protects neurons in mouse models of Parkinson's disease. Nature *447*,
582 1081–1086.

583 Dragicevic, E., Poetschke, C., Duda, J., Schlaudraff, F., Lammel, S., Schiemann, J., Fauler, M., Hetzel,
584 A., Watanabe, M., Luján, R., et al. (2014). Cav1.3 channels control D2-autoreceptor responses via
585 NCS-1 in substantia nigra dopamine neurons. Brain *137*, 2287-2302.

586 Fasano, C., Kortleven, C., and Trudeau, L.E. (2010). Chronic activation of the D2 autoreceptor inhibits
587 both glutamate and dopamine synapse formation and alters the intrinsic properties of mesencephalic
588 dopamine neurons in vitro. Eur J Neurosci *32*, 1433–1441.

589 Filtz, T.M., Artymyshyn, R.P., Guan, W., and Molinoff, P.B. (1993). Paradoxical regulation of
590 dopamine receptors in transfected 293 cells. Mol Pharmacol *44*, 371–379.

591 Fishburn, C.S., Elazar, Z., and Fuchs, S. (1995). Differential glycosylation and intracellular trafficking
592 for the long and short isoforms of the D2 dopamine receptor. J Biol Chem *270*, 29819–29824.

593 Foehring, R.C., Zhang, X.F., Lee, J.C.F., and Callaway, J.C. (2009). Endogenous Calcium Buffering
594 Capacity of Substantia Nigral Dopamine Neurons. J Neurophysiol *102*, 2326–2333.

595 Ford, C.P. (2014). The role of D2-autoreceptors in regulating dopamine neuron activity and
596 transmission. Neuroscience.

597 Ford, C.P., Gantz, S.C., Phillips, P.E.M., and Williams, J.T. (2010). Control of extracellular dopamine
598 at dendrite and axon terminals. Journal of Neuroscience *30*, 6975–6983.

599 Ford, C.P., Mark, G.P., and Williams, J.T. (2006) Properties and opioid inhibition of mesolimbic
600 dopamine neurons vary according to target location. Journal of Neuroscience *10*, 2788-2797.

601 Gantz, S.C., Bunzow, J.R., and Williams, J.T. (2013). Spontaneous inhibitory synaptic currents
602 mediated by a G protein-coupled receptor. Neuron *78*, 807–812.

603 Gantz, S.C., Ford, C.P., Neve, K.A., and Williams, J.T. (2011). Loss of Mecp2 in substantia nigra
604 dopamine neurons compromises the nigrostriatal pathway. Journal of Neuroscience *31*, 12629–12637.

605 Gantz, S.C., Levitt, E.S., Llamosas, N., Neve, K.A., and Williams, J.T. (2015). Depression of serotonin

606 synaptic transmission by the dopamine precursor L-DOPA. Cell Reports *12*, 944-954.

607 Giordano, T.P., Satpute, S.S., Striessnig, J., Kosofsky, B.E., and Rajadhyaksha, A.M. (2006). Up-
608 regulation of dopamine D(2)L mRNA levels in the ventral tegmental area and dorsal striatum of
609 amphetamine-sensitized C57BL/6 mice: role of Ca(v)1.3 L-type Ca(2+) channels. J Neurochem *99*,
610 1197–1206.

611 Goldberg, M.S., Pisani, A., Haburcak, M., Vortherms, T.A., Kitada, T., Costa, C., Tong, Y., Martella,
612 G., Tscherter, A., Martins, A., et al. (2005). Nigrostriatal dopaminergic deficits and hypokinesia
613 caused by inactivation of the familial Parkinsonism-linked gene DJ-1. Neuron *45*, 489–496.

614 Guzman, J.N., Sánchez-Padilla, J., Wokosin, D., Kondapalli, J., Ilijic, E., Schumacker, P.T., and
615 Surmeier, D.J. (2010). Oxidant stress evoked by pacemaking in dopaminergic neurons is attenuated by
616 DJ-1. Nature *468*, 696–700.

617 Hage, T.A., and Khaliq, Z.M. (2015). Tonic firing rate controls dendritic Ca2+ signaling and synaptic
618 gain in substantia nigra dopamine neurons. Journal of Neuroscience *35*, 5823–5836.

619 Henry, D.J., Greene, M.A., and White, F.J. (1989). Electrophysiological effects of cocaine in the
620 mesoaccumbens dopamine system: repeated administration. J Pharmacol Exp Ther *251*, 833–839.

621 Holroyd, K.B., Adrover, M.F., Fuino, R.L., Bock, R., Kaplan, A.R., Gremel, C.M., Rubinstein, M., and
622 Alvarez, V.A. (2015). Loss of Feedback Inhibition via D2 Autoreceptors Enhances Acquisition of
623 Cocaine Taking and Reactivity to Drug-Paired Cues. Neuropsychopharmacology *40*, 1495–1509.

624 Ito, K., Haga, T., Lameh, J., and Sadée, W. (1999). Sequestration of dopamine D2 receptors depends
625 on coexpression of G-protein-coupled receptor kinases 2 or 5. Eur. J. Biochem. *260*, 112–119.

626 Itokawa, M., Toru, M., Ito, K., Tsuga, H., Kameyama, K., Haga, T., Arinami, T., and Hamaguchi, H.
627 (1996). Sequestration of the short and long isoforms of dopamine D2 receptors expressed in Chinese
628 hamster ovary cells. Mol Pharmacol *49*, 560–566.

629 Jang, J.Y., Jang, M., Kim, S.H., Um, K.B., Kang, Y.K., Kim, H.J., Chung, S., and Park, M.K. (2011).
630 Regulation of dopaminergic neuron firing by heterogeneous dopamine autoreceptors in the substantia
631 nigra pars compacta. J Neurochem *116*, 966–974.

632 Jomphe, C., Tiberi, M., and Trudeau, L.-E. (2006). Expression of D2 receptor isoforms in cultured
633 neurons reveals equipotent autoreceptor function. Neuropharmacology *50*, 595–605.

634 Jones, S., Kornblum, J.L., and Kauer, J.A. (2000). Amphetamine blocks long-term synaptic depression
635 in the ventral tegmental area. J Neurosci *20*, 5575–5580.

636 Khan, Z.U., Mrzljak, L., Gutierrez, A., la Calle, de, A., and Goldman-Rakic, P.S. (1998). Prominence
637 of the dopamine D2 short isoform in dopaminergic pathways. Proc Natl Acad Sci USA *95*, 7731–7736.

638 Kramer, P.F., and Williams, J.T. (2015). Cocaine Decreases Metabotropic Glutamate Receptor
639 mGluR1 Currents in Dopamine Neurons by Activating mGluR5. Neuropsychopharmacology 1–7.

640 Lindgren, N., Usiello, A., Goiny, M., Haycock, J., Erbs, E., Greengard, P., Hokfelt, T., Borrelli, E., and
641 Fisone, G. (2003). Distinct roles of dopamine D2L and D2S receptor isoforms in the regulation of

protein phosphorylation at presynaptic and postsynaptic sites. Proc Natl Acad Sci USA *100*, 4305–4309.

Liu, Y.F., Civelli, O., Grandy, D.K., and Albert, P.R. (1992). Differential sensitivity of the short and long human dopamine D2 receptor subtypes to protein kinase C. J Neurochem *59*, 2311–2317.

Madhavan, A., Argilli, E., Bonci, A., and Whistler, J.L. (2013). Loss of D2 Dopamine Receptor Function Modulates Cocaine-Induced Glutamatergic Synaptic Potentiation in the Ventral Tegmental Area. Journal of Neuroscience *33*, 12329–12336.

Marinelli, M., and White, F.J. (2000). Enhanced vulnerability to cocaine self-administration is associated with elevated impulse activity of midbrain dopamine neurons. Journal of Neuroscience *20*, 8876–8885.

Marinelli, M., Cooper, D.C., Baker, L.K., and White, F.J. (2003). Impulse activity of midbrain dopamine neurons modulates drug-seeking behavior. Psychopharmacology (Berl) *168*, 84–98.

Morris, S.J., Itzhaki Van-Ham, I., Daigle, M., Robillard, L., Sajedi, N., and Albert, P.R. (2007). Differential desensitization of dopamine D2 receptor isoforms by protein kinase C: The importance of receptor phosphorylation and pseudosubstrate sites. Eur J Pharmacol *577*, 44–53.

Moyer, R.A., Wang, D., Papp, A.C., Smith, R.M., Duque, L., Mash, D.C., and Sadee, W. (2011). Intronic polymorphisms affecting alternative splicing of human dopamine D2 receptor are associated with cocaine abuse. Neuropsychopharmacology *36*, 753–762.

Neve, K.A., Ford, C.P., Buck, D.C., Grandy, D.K., Neve, R.L., and Phillips, T.J. (2013). Normalizing dopamine D2 receptor-mediated responses in D2 null mutant mice by virus-mediated receptor restoration: comparing D2L and D2S. Neuroscience *248*, 479–487.

Ng, G.Y., Varghese, G., Chung, H.T., Trogadis, J., Seeman, P., O'Dowd, B.F., and George, S.R. (1997). Resistance of the dopamine D2L receptor to desensitization accompanies the up-regulation of receptors on to the surface of Sf9 cells. Endocrinology *138*, 4199–4206.

Oomizu, S., Boyadjieva, N., and Sarkar, D.K. (2003). Ethanol and Estradiol Modulate Alternative Splicing of Dopamine D2 Receptor Messenger RNA and Abolish the Inhibitory Action of Bromocriptine on Prolactin Release From the Pituitary Gland. Alcohol Clin Exp Res *27*, 975–980.

Padgett, C.L., Lalive, A.L., Tan, K.R., Terunuma, M., Munoz, M.B., Pangalos, M.N., Martínez-Hernández, J., Watanabe, M., Moss, S.J., Luján, R., et al. (2012). Methamphetamine-evoked depression of GABA(B) receptor signaling in GABA neurons of the VTA. Neuron *73*, 978–989.

Perra, S., Clements, M.A., Bernier, B.E., and Morikawa, H. (2011). In Vivo Ethanol Experience Increases D2 Autoinhibition in the Ventral Tegmental Area. Neuropsychopharmacology *36*, 993–1002.

Pologruto, T.A., Sabatini, B.L., and Svoboda, K. (2003). ScanImage: flexible software for operating laser scanning microscopes. Biomed Eng Online *2*, 13.

Prou, D., Gu, W.J., Le Crom, S., Vincent, J.D., Salamero, J., and Vernier, P. (2001). Intracellular retention of the two isoforms of the D(2) dopamine receptor promotes endoplasmic reticulum disruption. Journal of Cell Science *114*, 3517–3527.

679 Puopolo, M., Raviola, E., and Bean, B.P. (2007). Roles of subthreshold calcium current and sodium
680 current in spontaneous firing of mouse midbrain dopamine neurons. Journal of Neuroscience *27*, 645–
681 656.

682 Radl, D., De Mei, C., Chen, E., Lee, H., and Borrelli, E. (2013). Each individual isoform of the
683 dopamine D2 receptor protects from lactotroph hyperplasia. Mol. Endocrinol. *27*, 953–965.

684 Roeper, J. (2013). Dissecting the diversity of midbrain dopamine neurons. Trends Neurosci *36*, 336–
685 342.

686 Sasabe, T., Furukawa, A., Matsusita, S., Higuchi, S., and Ishiura, S. (2007). Association analysis of the
687 dopamine receptor D2 (DRD2) SNP rs1076560 in alcoholic patients. Neurosci Lett *412*, 139–142.

688 Sharpe, A.L., Varela, E., Bettinger, L., and Beckstead, M.J. (2014). Methamphetamine Self-
689 Administration in Mice Decreases GIRK Channel-Mediated Currents in Midbrain Dopamine Neurons.
690 Int. J. Neuropsychopharmacol. *18*, pyu073–pyu073.

691 Smith, J.W., Fetsko, L.A., Xu, R., and Wang, Y. (2002). Dopamine D2L receptor knockout mice
692 display deficits in positive and negative reinforcing properties of morphine and in avoidance learning.
693 Nsc *113*, 755–765.

694 Starr, S., Kozell, L.B., and Neve, K.A. (1995). Drug-induced up-regulation of dopamine D2 receptors
695 on cultured cells. J Neurochem *65*, 569–577.

696 Thibault, D., Albert, P.R., Pineyro, G., and Trudeau, L.-E. (2011). Neurotensin triggers dopamine D2
697 receptor desensitization through a protein kinase C and beta-arrestin1-dependent mechanism. J Biol
698 Chem *286*, 9174–9184.

699 Usiello, A., Baik, J.H., Rougé-Pont, F., Picetti, R., Dierich, A., LeMeur, M., Piazza, P.V., and Borrelli,
700 E. (2000). Distinct functions of the two isoforms of dopamine D2 receptors. Nature *408*, 199–203.

701 Wang, Y., Xu, R., Sasaoka, T., Tonegawa, S., Kung, M.P., and Sankoorikal, E.B. (2000). Dopamine
702 D2 long receptor-deficient mice display alterations in striatum-dependent functions. Journal of
703 Neuroscience *20*, 8305–8314.

704 Wernicke, C., Hellmann, J., Finckh, U., and Rommelspacher, H. (2010). Chronic ethanol exposure
705 changes dopamine D2 receptor splicing during retinoic acid-induced differentiation of human SH-
706 SY5Y cells. Pharmacol Rep *62*, 649–663.

707 Wolf, M.E., White, F.J., Nassar, R., Brooderson, R.J., and Khansa, M.R. (1993). Differential
708 development of autoreceptor subsensitivity and enhanced dopamine release during amphetamine
709 sensitization. J Pharmacol Exp Ther *264*, 249–255.

710 Zhang, L.J., Lachowicz, J.E., and Sibley, D.R. (1994). The D2S and D2L dopamine receptor isoforms
711 are differentially regulated in Chinese hamster ovary cells. Mol Pharmacol *45*, 878–889.

712

713 **Figure 1.**

714 **When virally expressed in midbrain dopamine neurons, D2S and D2L function as autoreceptors.**

(**A**) Representative traces of whole-cell voltage clamp recordings, using a BAPTA-containing internal solution, of the outward current in D2S and D2L neurons induced by bath application of quinpirole (30 μM), which was reversed by sulpiride (600 nM). **(B)** The amplitude of quinpirole-induced currents in D2S and D2L neurons using BAPTA internal did not differ (*n*=12-14, unpaired *t* test), shown in reference to the amplitude of the quinpirole-induced currents in WT neurons (white line). **(C)** There was no difference between D2S and D2L in the decline of the D2 receptor-dependent current in the continued presence of quinpirole using BAPTA internal (two-way ANOVA). **(D-E)** Representative traces of spontaneous D2-sIPSCs mediated by D2S and D2L receptors, blocked by sulpiride. Inset boxes are shown enlarged in **(E)**. The frequency and amplitude of D2S- and D2L-sIPSCs were not analyzed since these parameters may be influenced by the expression of D2 receptors in presynaptic dopamine neurons, which cannot be confirmed. **(F)** The duration of D2S-sIPSCs and D2L-sIPSCs did not differ (*n*=84-100 sIPSCs, Mann-Whitney U test). ns indicates not significant.

Figure 2.

Weak intracellular calcium buffering reveals calcium-dependent desensitization of D2 autoreceptor-dependent GIRK currents in wild type dopamine neurons.

(**A**) Representative traces of whole-cell voltage clamp recordings of the outward current induced by bath application of quinpirole (10 μM) that was reversed by sulpiride (600 nM), using a BAPTA or EGTA-containing internal solution. **(B)** The amplitude of the quinpirole-induced current was larger using BAPTA than EGTA internal (*n*=15 each, unpaired *t* test). **(C-D)** The decline in quinpirole-induced current was faster using EGTA internal compared to BAPTA (**C**: two-way ANOVA followed by Bonferroni, **D**: unpaired *t* test) **(E)** Representative traces of whole-cell voltage clamp recordings of the outward current induced by bath application of baclofen (30 μM) which was reversed by CGP-55845 (200 nM), using BAPTA or EGTA internal. **(F)** The amplitude of the baclofen-induced current was larger using BAPTA than EGTA internal (*n*=14-16, unpaired *t* test). **(G-H)** There was no difference in the decline in baclofen-induced current recorded with EGTA and BAPTA internals (**G**: two-way ANOVA, **D**: unpaired *t* test). ns indicates not significant, *p<0.05, **p<0.01, ***p<0.001.

Figure 3.

Increasing resting free internal calcium does not enhance desensitization of D2 autoreceptor-dependent GIRK currents.

(**A**) The amplitude of the quinpirole (10 μM) -induced current using BAPTA+Ca^{2+} internal solution was not different from the amplitudes using BAPTA or EGTA internal solutions (*n*=7-15, ANOVA

748 followed by Bonferroni). **(B)** Increasing resting free calcium with BAPTA+Ca^{2+} had no effect on the
749 decline in quinpirole-induced current (two-way ANOVA). **(C)** Increasing resting free calcium with
750 BAPTA+Ca^{2+} internal decreased the amplitude of the baclofen (30 μM) -induced current, making it no
751 greater than the amplitude recorded using EGTA internal (ANOVA followed by Bonferroni). **(D)**
752 Increasing resting free calcium with BAPTA+Ca^{2+} had no effect on the decline in baclofen-induced
753 current (two-way ANOVA). Additional experiments that demonstrate BAPTA+Ca^{2+} internal increased
754 resting free calcium can be found in **Figure 3 - figure supplement 1.** ns indicates not significant,
755 **p<0.01, ***p<0.001.
756
757 **Figure 3 - figure supplement 1.**
758 **The positive modulator of the SK channel, NS309, produces an outward current when using the**
759 **BAPTA+Ca^{2+} internal solution.**
760 **(A)** Representative trace of whole-cell voltage clamp recordings of the outward current induced by
761 bath application of NS309 (10 μM), which was reversed by apamin (200 nM), using a BAPTA+Ca^{2+}
762 internal. **(B)** NS309 produced a current using a BAPTA+Ca^{2+}, but not BAPTA or EGTA internal
763 (*n*=5-6, ANOVA followed by Bonferroni). ns indicates not significant, ***p<0.001.
764
765 **Figure 4.**
766 **D2S but not D2L receptor-GIRK currents exhibit calcium-dependent desensitization.**
767 (**A**) Representative traces of whole-cell voltage clamp recordings of the outward current in D2S and
768 D2L neurons induced by bath application of quinpirole (30 μM) which was reversed by sulpiride (600
769 nM), using EGTA internal, compared with the BAPTA trace shown in **Figure 1A** (scaled and peak-
770 aligned). **(B, D)** Using EGTA internal, the decline in quinpirole-induced current was greater in D2S
771 than D2L neurons (**B**: two-way ANOVA followed by Bonferroni, **D**: *n*=16 each, one-way ANOVA
772 followed by Fisher's LSD). (**C**) The amplitude of quinpirole-induced currents in D2S and D2L
773 neurons using EGTA internal did not differ (*n*=16-17, unpaired *t* test), shown in reference to the
774 amplitude of the quinpirole-induced currents in WT neurons (white line). **(D)** In D2S neurons the
775 decline in quinpirole-induced current was greater using EGTA internal compared to BAPTA, but not
776 in D2L neurons (*n*=12-16, one-way ANOVA followed by Fisher's LSD). The time course of the
777 decline can be found in **Figure 4 - figure supplement 1. (E)** There was no difference in the decline in
778 baclofen-induced current recorded with EGTA or BAPTA internal in either splice variant (*n*=11-19,
779 one-way ANOVA). **(F)** In neurons from transgenic D2-Short mice**,** the amplitude of the quinpirole-
780 induced current was larger using BAPTA than EGTA internal (*n*=7-8, unpaired *t* test). **(G-H)**

781 Representative scaled and peak-aligned traces of whole-cell voltage clamp recordings from neurons
782 from transgenic D2-Short mice, of the outward currents induced by bath application of quinpirole (10
783 μM), which were reversed by sulpiride. The decline in quinpirole-induced current was greater using
784 EGTA internal compared to BAPTA (two-way ANOVA followed by Bonferroni). ns indicates not
785 significant, *p<0.05, **p<0.01, ***p<0.001.
786
787 **Figure 4 – figure supplement 1.**
788 **Time course of desensitization of D2 receptor splice variant-GIRK currents.**
789 **(A)** In D2S neurons**,** the decline in quinpirole (30 μM) -induced current was greater using EGTA
790 internal compared to BAPTA (*n*=10-16). (**B**) In D2L neurons**,** the decline in quinpirole-induced
791 current using EGTA internal was no different from BAPTA internal (*n*=10-16). Two-way ANOVAs
792 followed by Bonferroni). ns indicates not significant, *p<0.05, ***p<0.001.
793
794 **Figure 4 – figure supplement 2.**
795 **Expression and labeling of Flag-D2S receptors in dopamine neurons.**
796 (**A**) Representative confocal microscopy images of Flag-D2S receptors clustered on the soma,
797 dendrites, and spine-like structures of dopamine neurons, labeled by incubation of live slices in Alexa
798 Fluor-594 conjugated anti-Flag M1 antibody (red, Flag-D2S), then post-fixed and immunostained for
799 tyrosine hydroxylase (green, TH), scale bars: 1 μm (upper left inset) and 5 μm. (**B**) Representative
800 two-photon microscopy images of live dopamine neurons, where Flag-D2S receptors were labeled by
801 incubation of live slices in Alexa Fluor-594 conjugated anti-Flag M1 antibody (Flag-D2S), scale bars:
802 5 μm.
803
804 **Figure 5.**
805 **Depleting intracellular calcium stores differentially modifies D2S and D2L receptor-dependent**
806 **GIRK conductance.**
807 **(A)** In wild type neurons, CPA (10 μM, > 20 min) reduced the decline in the quinpirole-induced
808 current using EGTA internal and the effect was prevented with the use of BAPTA internal (*n*=11-15,
809 one-way ANOVA followed by Fisher's LSD). **(B)** CPA had no effect on the decline in baclofen-
810 induced current recorded with EGTA or BAPTA internal in wild type neurons (*n*=14-16, one-way
811 ANOVA). **(C)** In D2S**,** but not D2L neurons**,** CPA reduced the decline in quinpirole-induced current
812 using EGTA internal (*n*=6-16, one-way ANOVA followed by Fisher's LSD). **(D-E)** Submaximal D2
813 receptor-dependent outward currents were produced by iontophoretic application of dopamine once

every 50s while recording with EGTA internal (I-DA, arrows). **(D)** CPA (10 μM, 25-30 min) augmented I-DA in wild type neurons, shown in representative averaged traces (left) and grouped data (right, *n*=7). **(E)** CPA augmented I-DA in D2S and D2L neurons, shown in representative averaged traces (left) and grouped data (right). The augmentation by CPA was greater in D2L than D2S neurons (*n*=7-8, unpaired *t* test). The time course of the CPA-induced augmentation of I-DA can be found in **Figure 5 - figure supplement 1.** Baseline: mean amplitude of six I-DAs preceding CPA application, ns indicates not significant, *p<0.05, **p<0.01, ***p<0.001, and ‡ indicates significance over baseline (within-group comparison, paired *t* tests).

Figure 5 - figure supplement 1.

Prolonged CPA application enhances D2 receptor-dependent currents produced by exogenous dopamine.

(A) Submaximal D2 receptor-dependent outward currents (I-DA) were produced once every 50 s by iontophoretic application of dopamine while recording with EGTA internal. Prolonged CPA (10 μM) application enhanced I-DA in wild type (open circles), D2S (black circles), and D2L (black squares) neurons. Baseline: mean amplitude of six I-DAs preceding CPA application.

Figure 6.

Blocking L-type calcium channels differentially modifies D2S and D2L receptor-dependent GIRK conductance.

(A-B) In wild type neurons, isradipine (300 nM, > 20 min) had no significant effect on the decline in quinpirole-induced **(A)** and baclofen-induced current **(B)** recorded with EGTA and BAPTA internal (quinpirole: *n*=11-15, one-way ANOVA followed by Fisher's LSD; baclofen: *n*=12-16, one-way ANOVA). **(C)** In D2S**,** but not D2L neurons**,** isradipine reduced the decline in quinpirole-induced current using EGTA internal (*n*=6-16, one-way ANOVA followed by Fisher's LSD). **(D-E)** Submaximal D2 receptor-dependent outward currents were produced by iontophoretic application of dopamine once every 50s while recording with EGTA internal (I-DA, arrows). **(D)** Isradipine (300 nM, > 15 min) augmented I-DA in wild type neurons, shown in representative averaged traces (left) and grouped data (right, *n*=11). **(E)** Isradipine augmented I-DA in D2S and D2L neurons, shown in representative averaged traces (left) and grouped data (right). The augmentation by isradipine was greater in D2L than D2S neurons (*n*=6-11, unpaired *t* test). The time course of the isradipine-induced augmentation of I-DA can be found in **Figure 6 - figure supplement 1.** Baseline: mean amplitude of

six I-DAs preceding isradipine application, ns indicates not significant, *p<0.05, **p<0.01, and ‡ indicates significance over baseline (within-group comparison, paired *t* tests).

Figure 6 - figure supplement 1.

Prolonged isradipine application enhances D2 receptor-dependent currents produced by exogenous dopamine.

(A) Submaximal D2 receptor-dependent outward currents (I-DA) were produced once every 50 s by iontophoretic application of dopamine while recording with EGTA internal. Prolonged isradipine (300 nM) application enhanced I-DA in wild type (open circles), D2S (black circles), and D2L (black squares) neurons. Baseline: mean amplitude of six I-DAs preceding isradipine application.

Figure 7.

Effects of a single *in vivo* cocaine exposure on calcium-dependent D2 autoreceptor desensitization.

(A) In neurons from cocaine-treated wild type mice using EGTA internal, the quinpirole-induced current declined less compared to naïve/saline-treated mice, to a level comparable to the decline recorded with BAPTA internal. Cocaine exposure did not alter the decline in the quinpirole-induced current when measured with BAPTA internal (*n*=11-26). (**B**) In D2L neurons after *in vivo* cocaine exposure, there was no difference in the decline in quinpirole-induced current recorded with EGTA or BAPTA internal (*n*=6-7). **(C-D)** In neurons from (**C**) AAV-D2S and (**D**) transgenic D2-Short mice, the decline in quinpirole-induced current was still greater using EGTA internal compared to BAPTA after *in vivo* cocaine exposure (**C**: *n*=10 each, **D**: *n*=8-9). **(D-E)** Co-expression of both splice variants by (**D**) viral expression of D2L in transgenic D2-Short mice and (**E**) infection with a mixture of AAV-D2S and AAV-D2L removed the calcium-dependence of the decline in the quinpirole-induced current (**D**: *n*=5-8, **E**: *n*=6-9) and there was no change after *in vivo* cocaine (**E**: *n*=7-9). **(F)** Previous cocaine exposure had no effect on the decline in baclofen-induced current recorded with EGTA or BAPTA internal in wild type neurons (*n*=13-27). Comparisons were made with one-way ANOVAs followed when p<0.05 by Fisher's LSD. ns indicates not significant, *p<0.05, **p<0.01, ***p<0.001.

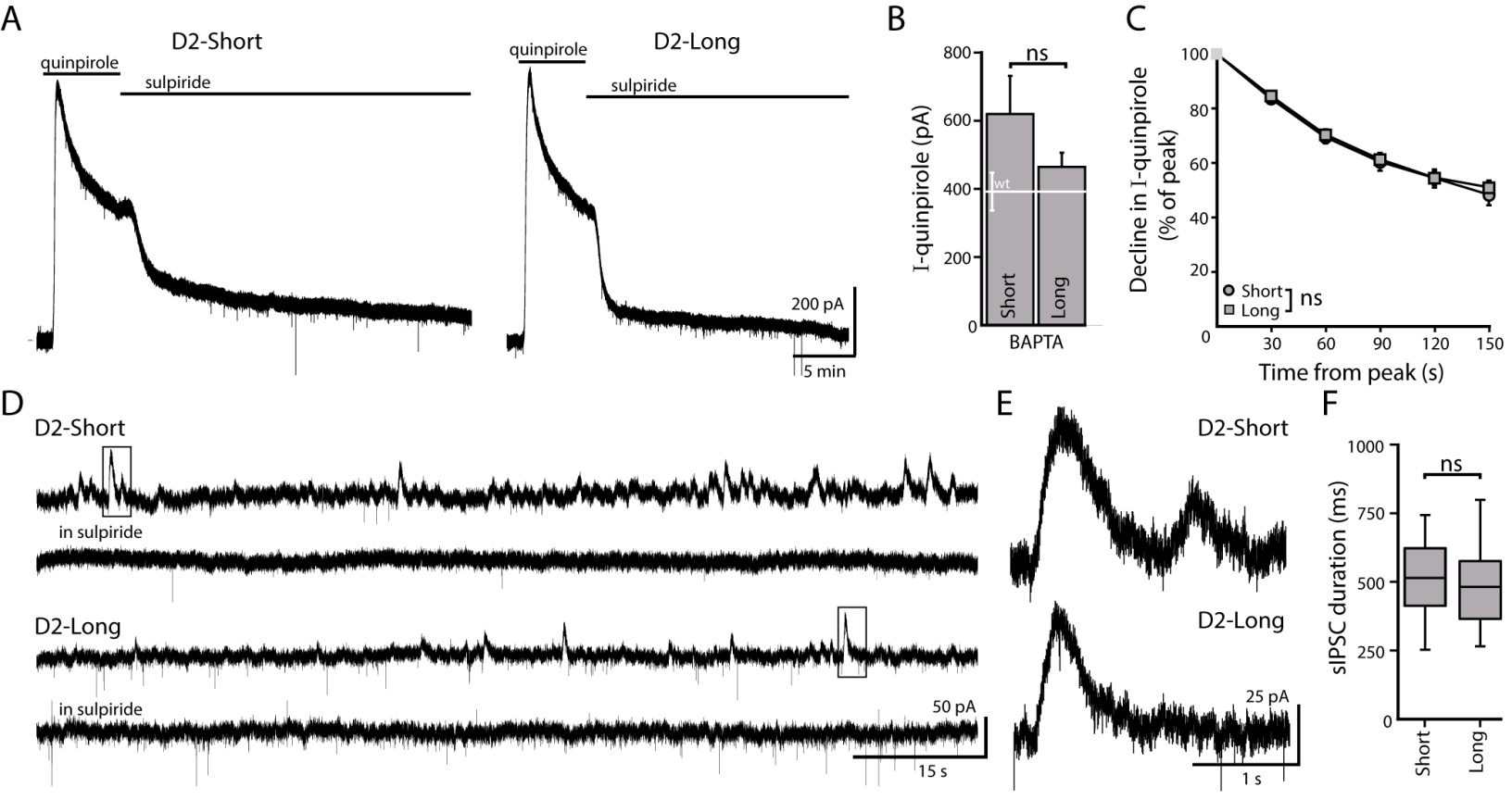
A
D2-Short
quinpirole
sulpiride
D2-Long
quinpirole
sulpiride
200 pA
5 min
B
ns
800
600
400
200
0
I-quinpirole (pA)
wt
Short
Long
BAPTA
C
100
80
60
40
20
0
Decline in I-quinpirole (% of peak)
Short
Long
ns
30
60
90
120
150
Time from peak (s)
D
D2-Short
in sulpiride
D2-Long
in sulpiride
50 pA
15 s
E
D2-Short
D2-Long
25 pA
1 s
F
1000
750
500
250
0
sIPSC duration (ms)
ns
Short
Long

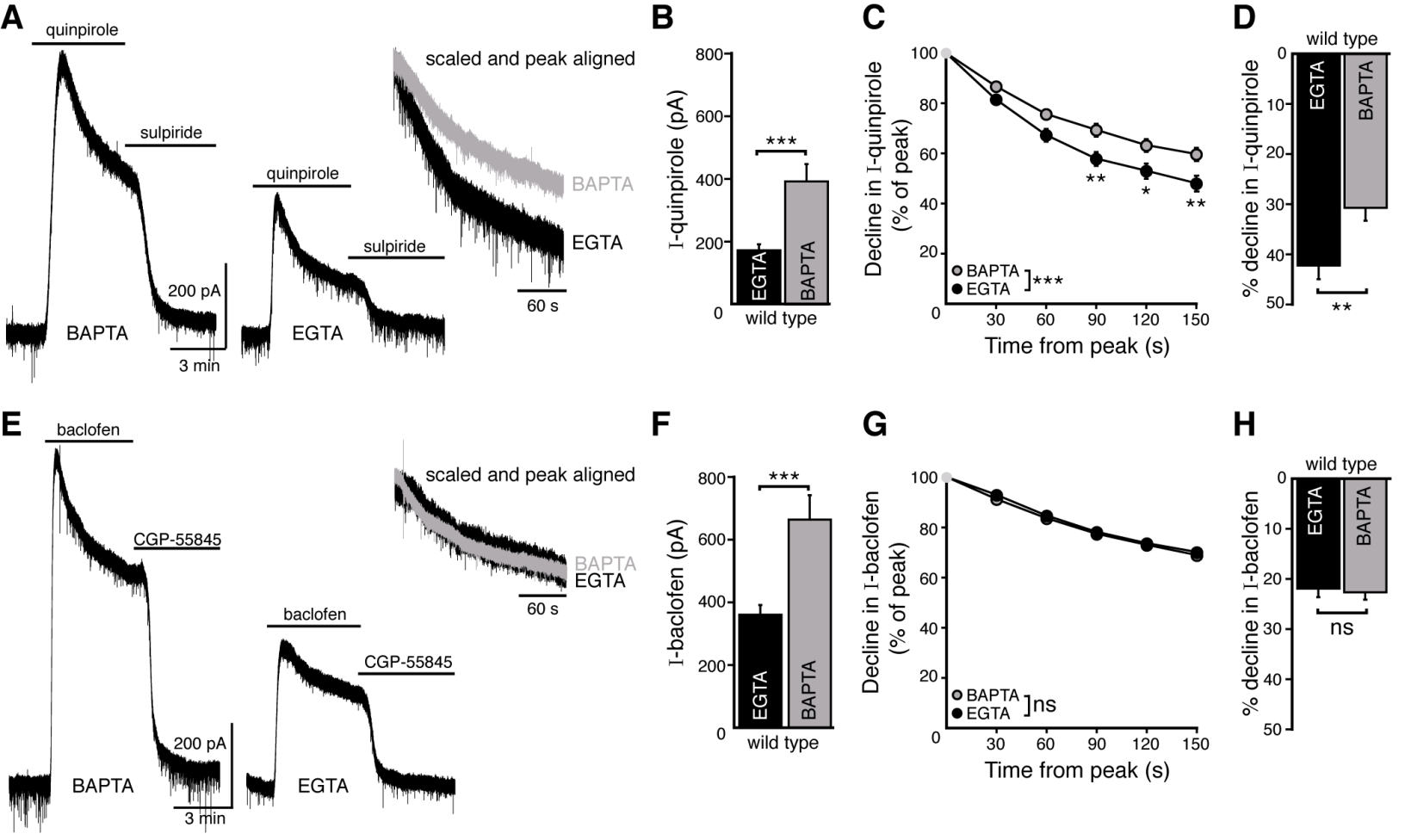
A
quinpirole
sulpiride
200 pA
BAPTA
3 min
quinpirole
sulpiride
EGTA
scaled and peak aligned
BAPTA
EGTA
60 s
B
I-quinpirole (pA)
800
600
400
200
0
***
EGTA
BAPTA
wild type
C
Decline in I-quinpirole (% of peak)
100
80
60
40
20
0
BAPTA
EGTA
***
**
*
**
30
60
90
120
150
Time from peak (s)
D
wild type
% decline in I-quinpirole
0
10
20
30
40
50
EGTA
BAPTA
**
E
baclofen
CGP-55845
200 pA
BAPTA
3 min
baclofen
CGP-55845
EGTA
scaled and peak aligned
BAPTA
EGTA
60 s
F
I-baclofen (pA)
800
600
400
200
0
***
EGTA
BAPTA
wild type
G
Decline in I-baclofen (% of peak)
100
80
60
40
20
0
BAPTA
EGTA
ns
30
60
90
120
150
Time from peak (s)
H
wild type
% decline in I-baclofen
0
10
20
30
40
50
EGTA
BAPTA
ns

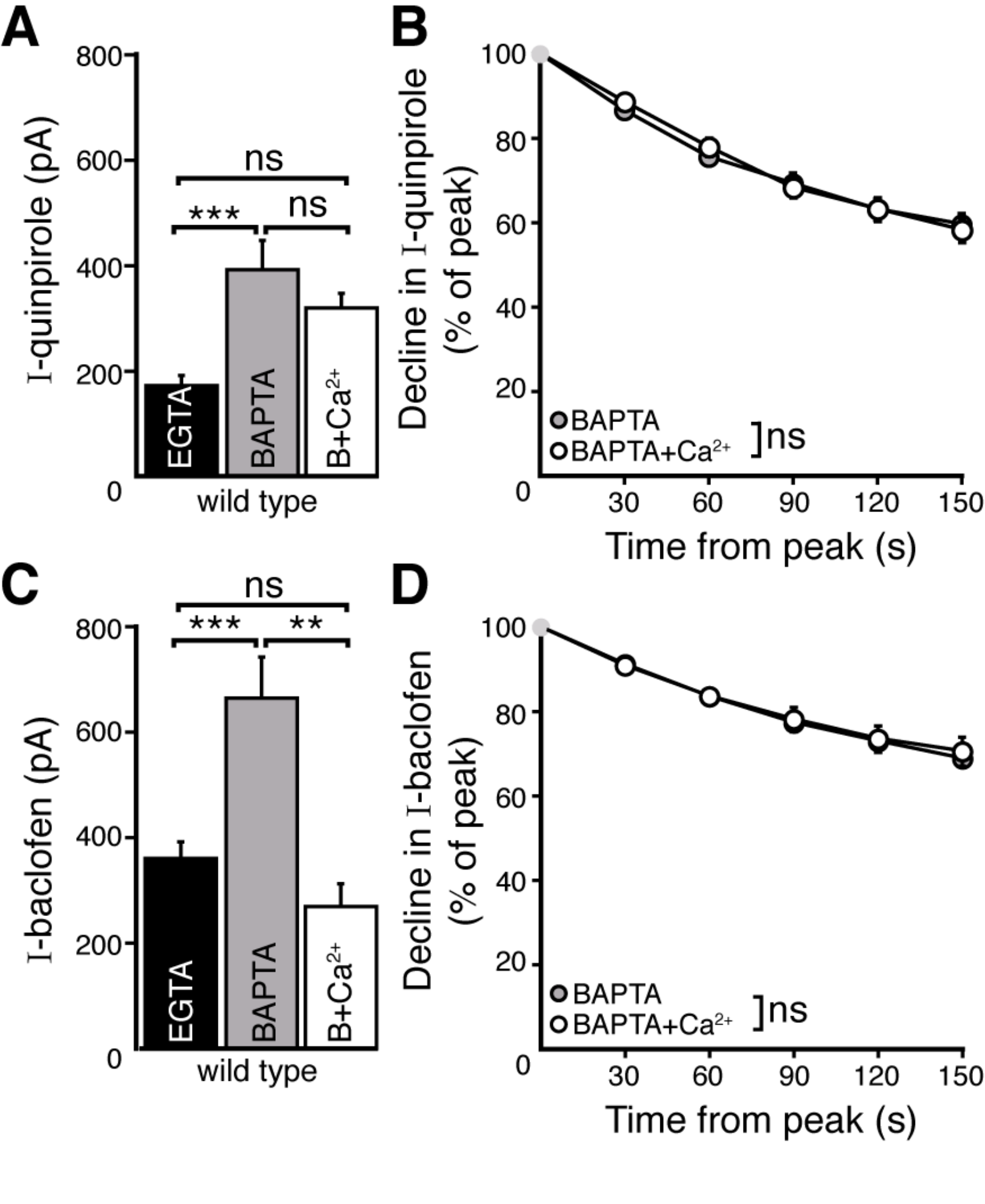
A
I-quinpirole (pA)
800
600
400
200
0
ns
***
ns
EGTA
BAPTA
B+Ca2+
wild type
B
Decline in I-quinpirole (% of peak)
100
80
60
40
20
0
BAPTA
BAPTA+Ca2+
ns
30
60
90
120
150
Time from peak (s)
C
I-baclofen (pA)
800
600
400
200
0
ns
***
**
EGTA
BAPTA
B+Ca2+
wild type
D
Decline in I-baclofen (% of peak)
100
80
60
40
20
0
BAPTA
BAPTA+Ca2+
ns
30
60
90
120
150
Time from peak (s)

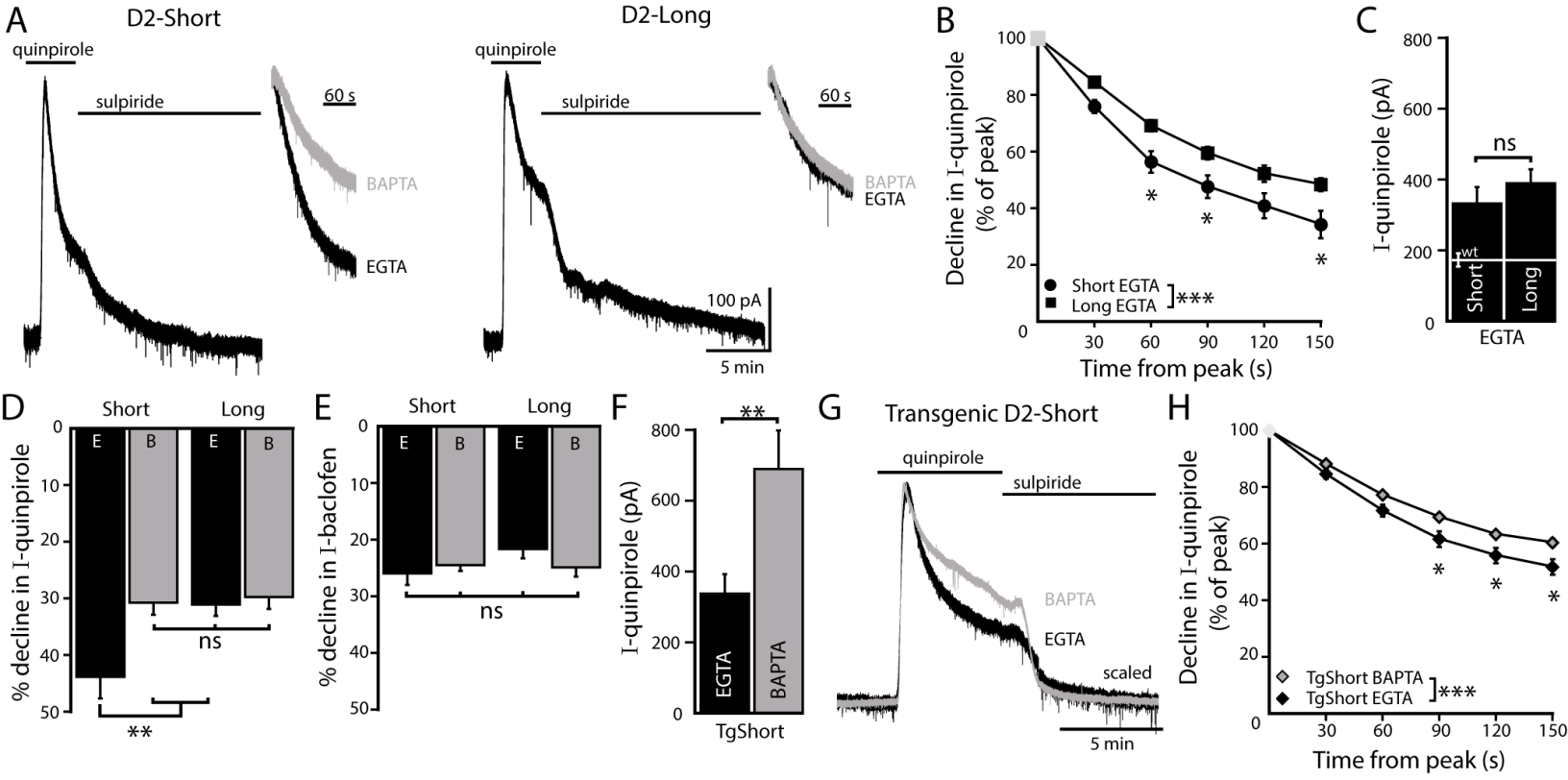
A
D2-Short
quinpirole
sulpiride
60 s
BAPTA
EGTA
D2-Long
quinpirole
sulpiride
60 s
BAPTA
EGTA
100 pA
5 min
B
Decline in I-quinpirole (% of peak)
Short EGTA
Long EGTA
***
Time from peak (s)
C
I-quinpirole (pA)
ns
wt
Short
Long
EGTA
D
Short
Long
% decline in I-quinpirole
E
B
ns
**
E
Short
Long
% decline in I-baclofen
ns
F
**
I-quinpirole (pA)
EGTA
BAPTA
TgShort
G
Transgenic D2-Short
quinpirole
sulpiride
BAPTA
EGTA
scaled
5 min
H
Decline in I-quinpirole (% of peak)
TgShort BAPTA
TgShort EGTA
***
Time from peak (s)

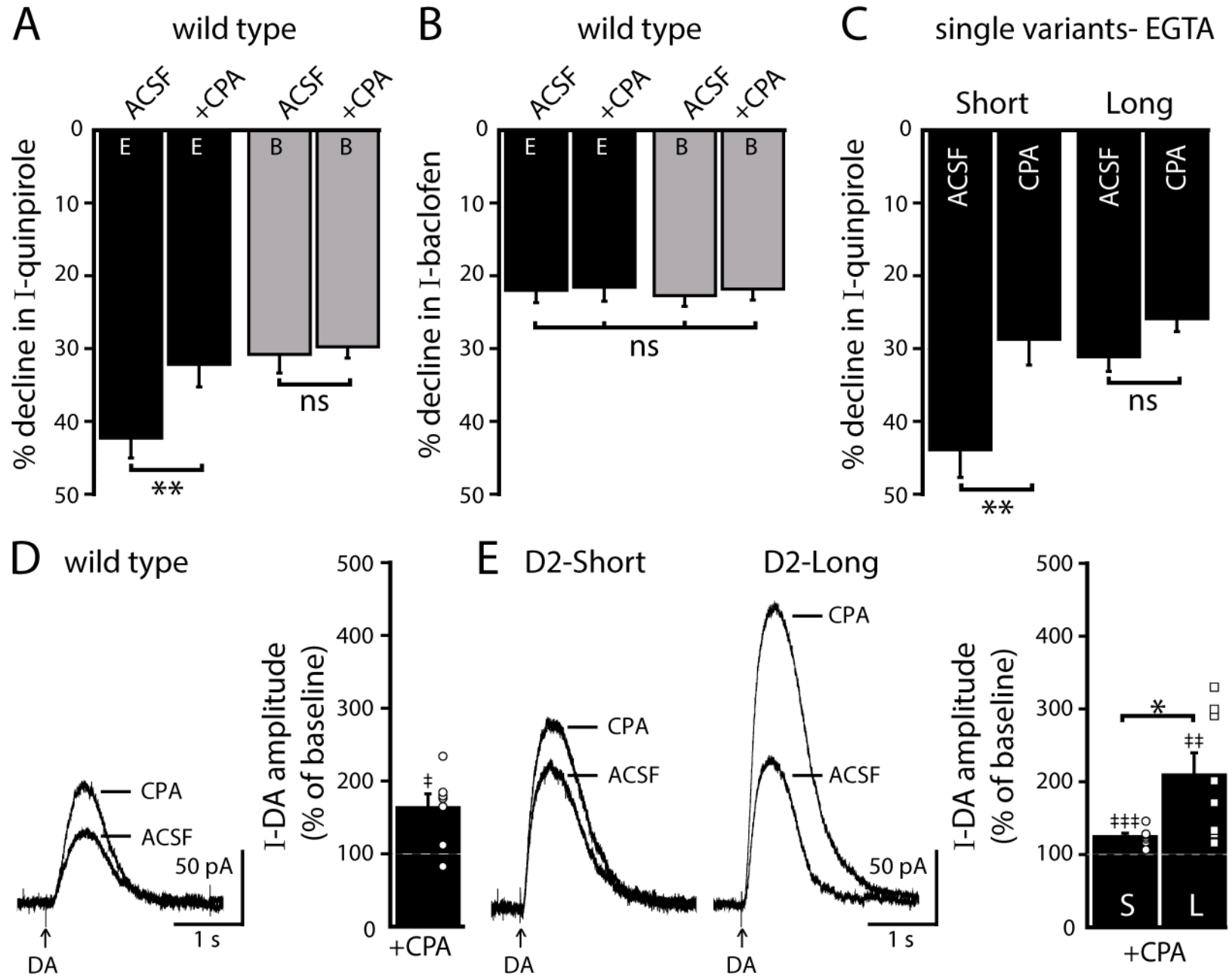
A
wild type
ACSF
+CPA
ACSF
+CPA
E
E
B
B
% decline in I-quinpirole
0
10
20
30
40
50
ns
**
B
wild type
ACSF
+CPA
ACSF
+CPA
E
E
B
B
% decline in I-baclofen
0
10
20
30
40
50
ns
C
single variants- EGTA
Short
Long
ACSF
CPA
ACSF
CPA
% decline in I-quinpirole
0
10
20
30
40
50
ns
**
D
wild type
CPA
ACSF
50 pA
1 s
DA
I-DA amplitude (% of baseline)
500
400
300
200
100
0
+CPA
E
D2-Short
D2-Long
CPA
ACSF
CPA
ACSF
50 pA
1 s
DA
DA
I-DA amplitude (% of baseline)
500
400
300
200
100
0
*
S
L
+CPA

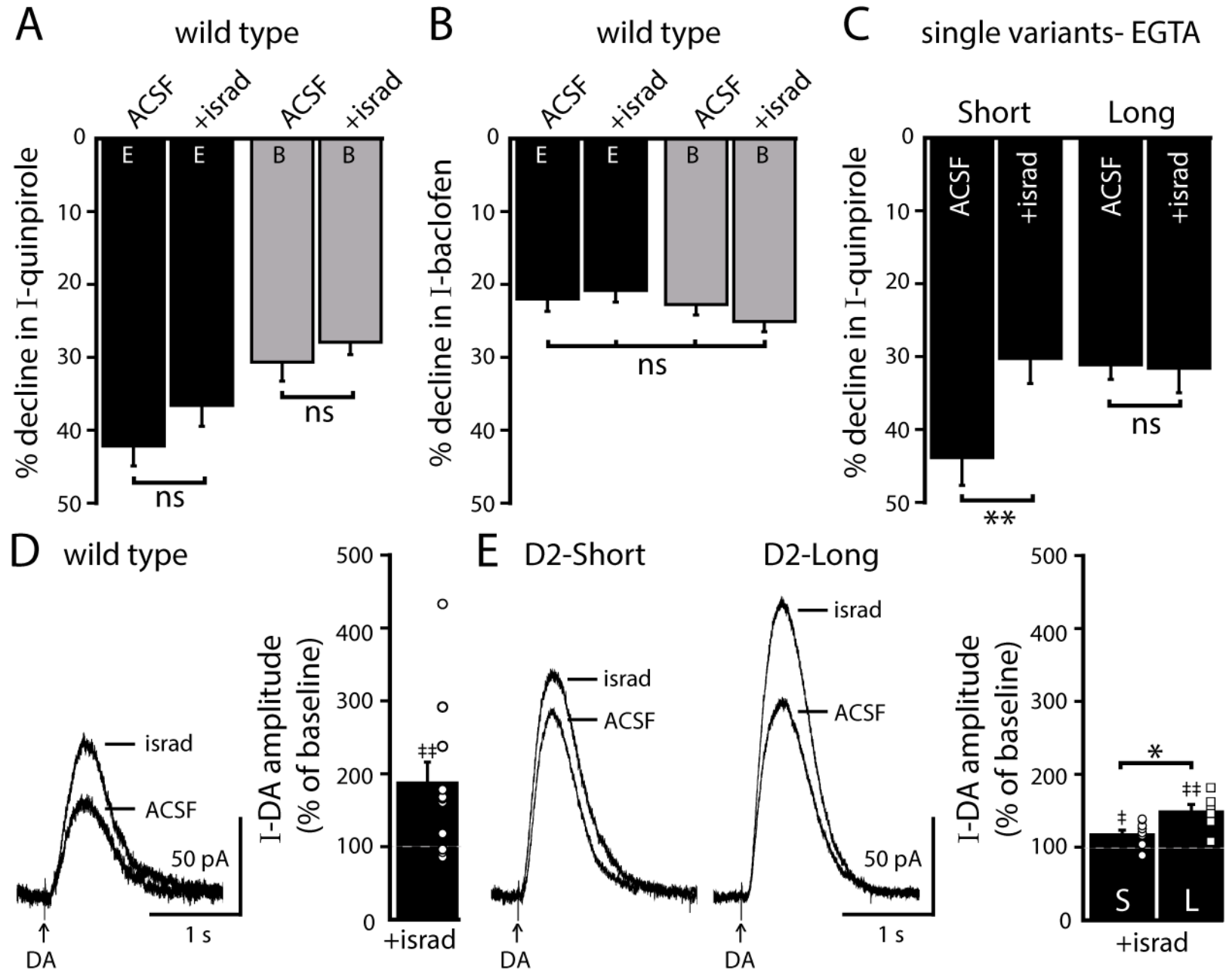
A
wild type
ACSF
+israd
ACSF
+israd
E
E
B
B
% decline in I-quinpirole
0
10
20
30
40
50
ns
ns
B
wild type
ACSF
+israd
ACSF
+israd
E
E
B
B
% decline in I-baclofen
0
10
20
30
40
50
ns
C
single variants- EGTA
Short
Long
ACSF
+israd
ACSF
+israd
% decline in I-quinpirole
0
10
20
30
40
50
**
ns
D
wild type
israd
ACSF
50 pA
1 s
DA
I-DA amplitude (% of baseline)
500
400
300
200
100
0
+israd
E
D2-Short
D2-Long
israd
ACSF
israd
ACSF
50 pA
1 s
DA
DA
I-DA amplitude (% of baseline)
500
400
300
200
100
0
*
S
L
+israd

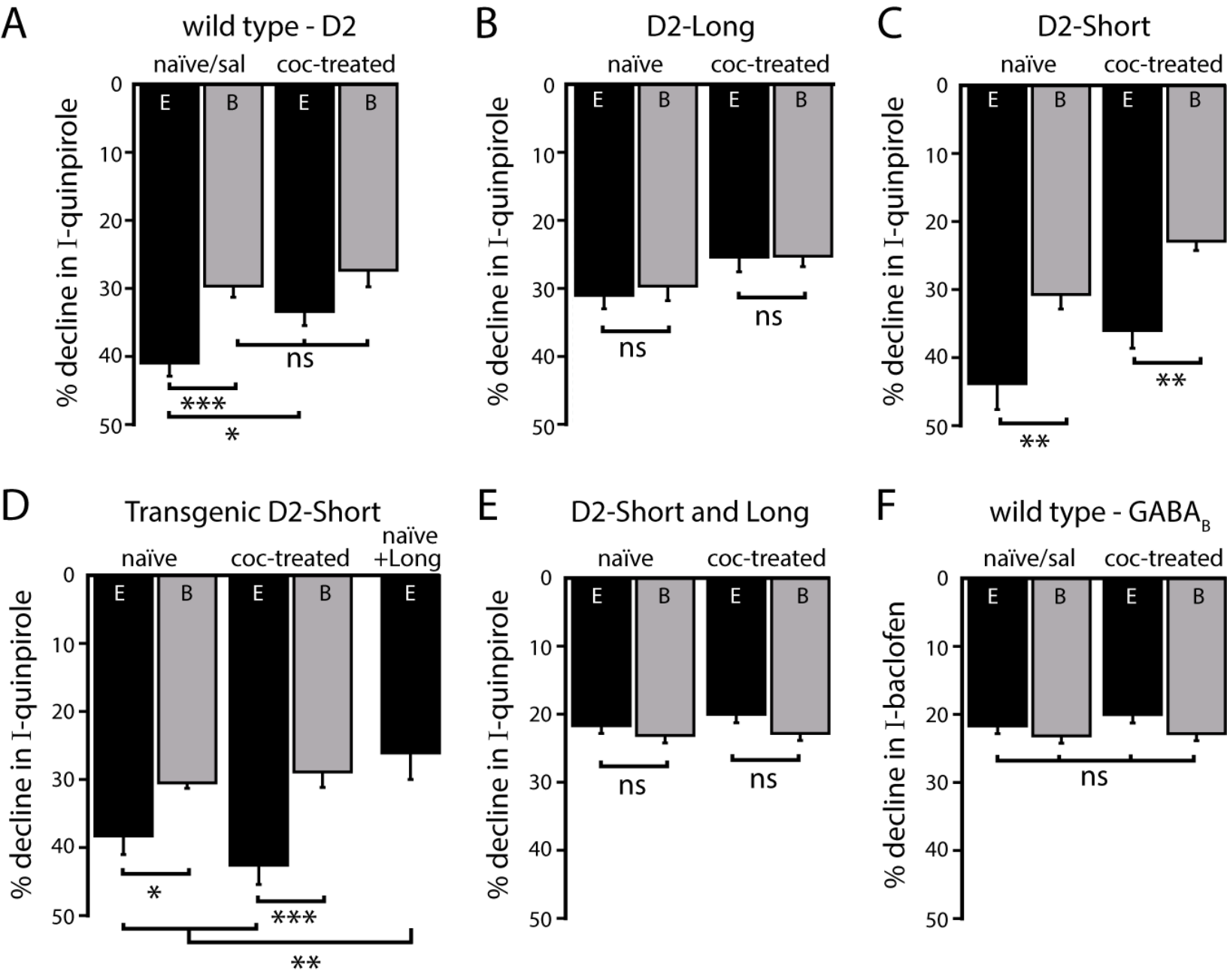
A
wild type - D2
naïve/sal
coc-treated
% decline in I-quinpirole
E
B
ns
***
*
B
D2-Long
naïve
coc-treated
ns
ns
C
D2-Short
naïve
coc-treated
**
**
D
Transgenic D2-Short
naïve
coc-treated
naïve +Long
*
***
**
E
D2-Short and Long
naïve
coc-treated
ns
ns
F
wild type - GABA$_B$
naïve/sal
coc-treated
% decline in I-baclofen
ns
0
10
20
30
40
50